

January 2007, revised July 2007

FTPI-MINN-07/01
UMN-TH-2534/07

Chiral Lattice Gauge Theories and The Strong Coupling Dynamics of a Yukawa-Higgs Model with Ginsparg-Wilson Fermions

JOEL GIEDT¹

*William I. Fine Theoretical Physics Institute
University of Minnesota
Minneapolis, MN 55455, USA*

and

ERICH POPPITZ

*Department of Physics
University of Toronto
Toronto, ON M5S 1A7, Canada*

giedtj@rpi.edu, poppitz@physics.utoronto.ca

Abstract:

The Yukawa-Higgs/Ginsparg-Wilson-fermion construction of chiral lattice gauge theories described in hep-lat/0605003 uses exact lattice chirality to decouple the massless chiral fermions from a mirror sector, whose strong dynamics is conjectured to give cutoff-scale mass to the mirror fermions without breaking the chiral gauge symmetry. In this paper, we study the mirror sector dynamics of a two-dimensional chiral gauge theory in the limit of strong Yukawa and vanishing gauge couplings, in which case it reduces to an XY model coupled to Ginsparg-Wilson fermions. For the mirror fermions to acquire cutoff-scale mass it is believed to be important that the XY model remain in its “high temperature” phase, where there is no algebraic ordering—a conjecture supported by the results of our work. We use analytic and Monte-Carlo methods with dynamical fermions to study the scalar and fermion susceptibilities, and the mirror fermion spectrum. Our results provide convincing evidence that the strong dynamics does not “break” the chiral symmetry (more precisely, that the mirror fermions do not induce algebraic ordering in two-dimensions), and that the mirror fermions decouple from the infrared physics.

¹Present address: Rensselaer Polytechnic Institute, Department of Physics, Applied Physics and Astronomy, 110 Eighth Street, Troy, NY 12180, USA

1 Introduction and summary

1.1 Motivation

The study of strong-coupling chiral gauge dynamics is an outstanding problem of great interest, both on its own and for its possible relevance to phenomenology. Whereas the standard model of elementary particle physics is a weakly coupled chiral gauge theory, additional strong chiral gauge dynamics at (multi-) TeV scales may be responsible for breaking the electroweak symmetry and fermion mass generation. Various tools are currently available for the study of the strong-coupling behavior of chiral gauge theories. For instance, one has 't Hooft's anomaly matching and most attractive channel arguments. These are complemented by the “power of holomorphy” in supersymmetric theories. Scaling arguments and effective NJL-like models, both using results from QCD as a stepping stone, have also been employed extensively. (Large- N expansions, including the recently considered gravity duals in the AdS/CFT (AdS/QCD) framework, do not usefully apply to chiral gauge theories.) None of these approaches represents a “first principles” method, with an accuracy that can be systematically improved. Thus, the space-time lattice regularization remains, to this day, the only way to advance our limited knowledge of strong chiral gauge dynamics.

During the past two decades, since the work [1] of Ginsparg and Wilson (GW), there has been significant progress in understanding chiral symmetries on the lattice [2–6] (further references are given in the reviews [7, 8], while [9, 10] contain more recent work). However, the lattice formulation of chiral gauge theories is still a largely unsolved problem, although there were some advances and promising two-dimensional numerical results using the original overlap Weyl determinant [11]. The fact that a general formulation is lacking, along with the natural expectation that the lattice definition of a chiral gauge theory is not unique, indicates that the exploration of the various existing formulations, of their interconnections, as well as of novel constructions of chiral lattice gauge theories are both warranted and worthwhile.

This paper is devoted to a study of a recently proposed construction of lattice chiral gauge theories [12]. It combines the GW exact lattice chiral symmetry with earlier ideas of strong coupling Higgs-Yukawa dynamics on the lattice, see [13–17] and references therein. The essence of the proposal is that the exact lattice chiral symmetry may allow an old dream to be realized: that the mirror partners of the chiral massless fermions can be decoupled, without breaking the gauge symmetry. The decoupling of the mirrors is possible in the strong-Yukawa symmetric phases of lattice fermion-Higgs models, where the fermions have cutoff-scale mass without breaking the chiral symmetry.

The mechanism of mass generation without chiral symmetry breaking operative in strongly-coupled lattice theories has been known for some time:¹ at strong Yukawa coupling, the charged mirror fermions form neutral bound states with the charged scalars; these bound states can pair up with other neutral mirror fermions, composite or elementary, to obtain mass without breaking the chiral symmetry.

The construction of [12] gives an explicit definition of a local lattice action and measure. The global symmetry Ward identities, exact or anomalous, are precisely as in the target continuum theory, which sets the proposal apart from earlier constructions aiming to decouple the mirror

¹In the two-dimensional context this mechanism was elucidated by Witten [18] via bosonization. In the case of four-dimensional strong four-Fermi interactions on the lattice, it was part of the proposal of Eichten and Preskill [13] to formulate chiral gauge theories on the lattice. In the context of strong-Yukawa lattice models it was discussed in [14–17].

fermions. We believe that these desirable features are alone sufficient to motivate further study of the proposal.

The lattice model of [12] will give rise to an unbroken chiral gauge theory only if there exists a strong-Yukawa phase with an unbroken gauge symmetry, massless chiral charged fermion spectrum, and massive mirror fermions. Because the construction makes use of the somewhat complicated exact lattice chiral symmetry, implemented via the Neuberger-Dirac operator [4], a strictly analytic approach—e.g., a strong-coupling expansion as used in [13–16]—to establishing the existence of the desired strong-coupling phase appears out of reach. The purpose of this paper is to provide evidence, using a semi-analytic approach that computes the leading terms of the strong-coupling Yukawa expansion by Monte Carlo estimation, for the existence of the strong-coupling symmetric phase with a massive mirror fermion spectrum.

1.2 Organization and summary of main results

In Section 2, we begin with a review of the proposal and of the arguments leading us to expect that an unbroken gauge theory with a chiral spectrum of charged fermions emerges in the infrared.² We present the construction on the example of a two-dimensional chiral $U(1)$ theory, the well-known “345” theory. While the proposed lattice action can also be written in four dimensions, the simplicity of the analytical analysis, and especially, the relative ease of the numerical analysis, restricts the present study of the dynamics to the two-dimensional case.

Of course, due to the special properties of two-dimensional theories, the exact $U(1)$ symmetry cannot be spontaneously broken [19]. However, the gauge boson would acquire a large mass (relative to the gap induced by the Schwinger mechanism) in the quasi-ordered phase, which is analogous to spontaneous symmetry breaking in the four-dimensional case. It is for this reason that here, and in several places below, we shall, with some abuse of language, use the term “broken” phase to refer to the low-temperature phase of the two-dimensional XY model, instead of the more appropriate algebraically- or quasi-ordered phase. Similarly, we will sometimes refer to the high-temperature disordered phase as the “symmetric” or “unbroken” phase and will take the liberty to omit the quotation marks.

In Section 3, we formulate a “toy” version of the model, simple enough to be subjected to extensive analytical and numerical tests. The main focus of this paper is the Higgs-Yukawa dynamics of this “toy” theory at strong Yukawa coupling and vanishing gauge coupling—the relevant limit to approach the continuum theory. The importance of this analysis is that it addresses precisely the question: is there a symmetric phase with a massless chiral spectrum of charged fermions in this model? A positive answer to this question is crucial for the viability of the proposal; a negative one would imply that the proposal should be abandoned.

We begin the analysis in Section 3.2, where we show that the partition function of our model factorizes into a product of “light” and “mirror” partition functions. We work out the splitting of the fermion measure into a product of positive and negative GW-chirality measures, using Neuberger’s Dirac operator, and the resulting factorization of the partition function; we give the technical details pertinent to this analysis in Appendix A. The factorization of the partition function is a unique feature of the GW-fermion Higgs-Yukawa theory that makes it distinct from other Higgs-Yukawa approaches, notably the “waveguide” models [20–22].

²See also Section IV in [12].

The exact light/mirror split of the partition function at $g = 0$ allows us to further concentrate entirely on the study of the dynamics of the mirror fermion-Higgs theory. The $g = 0$ mirror fermion-Higgs theory of the “toy” model is equivalent to the two-dimensional XY model (see, e.g., [23]) in the high-temperature disordered phase, $\kappa < \kappa_c$, deformed by the addition of fermions strongly coupled to the spins.

We next ask, in Section 3.3, whether a strong coupling symmetric phase of the mirror-fermion Higgs-Yukawa theory exists. We begin by noting that at strong Yukawa coupling the mirror fermion determinant is positive for arbitrary Higgs field background, provided the ratio of the Majorana to Dirac Yukawa couplings $h > 1$. The positivity of the fermion determinant permits us to numerically study the effect of mirror fermion “loops” on the Higgs field dynamics in the symmetric phase (i.e., at small Higgs kinetic term κ).³

We demonstrate the existence of a symmetric phase at strong Yukawa coupling by studying the scalar susceptibility in Section 3.3.1, the Binder cumulant—a quantity [24] probing higher-order correlations—in Section 3.3.2, the vortex density in Section 3.3.3, and the fermion bilinear susceptibilities in Section 3.3.4. We use numerical simulations to investigate the behavior of the various susceptibilities for different values of κ and h on lattices of size $N^2 = 4^2, 8^2, 16^2$. The Monte Carlo techniques we use are described in Appendix C. The combined study of the scalar and fermion bilinear order parameters and their scaling with N presents ample evidence that the theory is in the symmetric phase at strong Yukawa coupling to the mirror fermions, provided $h > 1$.

For $h \leq 1$, still at small κ , we find evidence for criticality as appropriate in the low-temperature phase of the XY -model, where the susceptibility increases with the volume of the system; concurrently we find that the mirror fermion spectrum contains massless modes and that the vortex density decreases rapidly as h approaches unity from above, as in the Berezinski-Kosterlitz-Thouless transition to the low-temperature phase.

In summary, our results of Section 3.3 show that the strong coupling symmetric phase exists and thus the $U(1)$ symmetry—the global part of the gauge group—is unbroken. This result also implies that no fine-tuning is required in order to keep the theory in the symmetric phase (after gauging—keeping the gauge boson perturbatively massless⁴) at strong Yukawa coupling. This is in contrast with a naive perturbative argument which would, at large Yukawa coupling, imply a large backreaction of the mirror fermions on the Higgs dynamics, thus requiring fine-tuning of potentially many terms to keep the model in the symmetric phase. The small backreaction of the fermions on the Higgs dynamics at large Yukawa is, however, consistent with the qualitative strong-coupling arguments of Section 2 and [12].

The next question we address is the mirror fermion spectrum in the symmetric phase. In Section 3.4, we study the spectrum of both charged and neutral mirror fermions and show that they are all massive in the strong Yukawa symmetric phase, for h greater than unity.

We note that, to the best of our knowledge, this is the first strong-Yukawa/Higgs construction within the framework of the “waveguide-like” (or Wilson-Yukawa) approaches to lattice chiral gauge theories that successfully yields a chiral massless spectrum of fermions at $g = 0$. Previous Yukawa approaches have failed to yield a chiral light spectrum of charged fermions already at the quenched, $g = 0$, level, see [21,22] and references therein. (The only exception that we know of is the quenched study [25] of a theory that is in some respects similar to our toy model, in the framework of the “two-

³Actually, “loops” is a bit of a misnomer since our large Yukawa expansion is just the opposite of the usual loop expansion. Our results are in that sense nonperturbative.

⁴Setting aside the effects of the Schwinger mechanism.

cutoff” construction of [26]. The advantages of the model that we study here is that, unlike [25], it exactly preserves the symmetries of the target theory and the mirror fermions exactly decouple.) In our construction, the crucial ingredient that leads to a chiral spectrum is the decoupling, due to the exact lattice chirality, of the light chiral fermions from the strong Higgs-Yukawa dynamics of the mirror sector. It is the main feature that distinguishes our models from earlier “Wilson-Yukawa” or “waveguide” constructions.

1.3 Conclusions and outlook

Our main results are:

1. We have shown that exact lattice chirality can be used to decouple the massless chiral fermions from a mirror sector. The light-mirror split of the fermion partition function is given in Appendix A.
2. We have given numerical evidence that the strong Yukawa dynamics of the mirror sector gives cutoff-scale mass to the mirror fermions, without breaking the gauge symmetry (i.e. without inducing algebraic ordering in two dimensions).
3. We have found that, at strong Yukawa coupling, the main effect of the mirror fermions on the XY model to which they are coupled is to renormalize the hopping parameter κ to smaller values—deeper into the “high temperature” phase—provided $h > 1$. For instance, in the XY model coupled to fermions, the vortex density is higher, and the susceptibility is lower, than in corresponding pure XY model. This conclusion is further supported by the step function centered on $h = 1$ that develops in the Binder cumulant, extrapolated to the $N \gg 1$ limit.

Our results show that our proposed formulation of chiral lattice gauge theories satisfies a first check on its viability: the strong Yukawa dynamics produces heavy mirrors without breaking the gauge symmetry.

Clearly, the results of this paper encourage further inquiry:

- The toy model studied here gives rise to a would-be anomalous massless fermion spectrum in a trivial ($U = 1$) gauge background. The issue of gauge anomalies in models where non-gauge dynamics in the mirror sector is introduced to decouple the mirrors was recently studied in [27]. As explained there, in the anomalous case a result for the mirror spectrum at $U = 1$ can not be used to infer the spectrum at $U \neq 1$, since for an anomalous fermion content the mirror fermion partition function is not a smooth function exactly at $U = 1$ and the split of the partition function into “light” and “mirror” is not consistent in this case (this is how the non-gauge mirror sector dynamics introduced to decouple mirrors is required to obey the anomaly free condition). Clearly, the next important step is to study the mirror dynamics in an anomaly-free model, like the 345 model. See also the discussion in the Addendum of ref. [27].
- In the anomaly free case, we have reason to believe that our results will hold for nonvanishing gauge coupling, since the mirror-fermion/ XY -model physics is at the ultraviolet scale, where the gauge coupling is weak. As shown in [27], the mirror partition function is a smooth function of the gauge background in the anomaly free case and a result showing that the

mirror fermions decouple at $U = 1$ should persist for small nontrivial gauge background, e.g. in perturbation theory with respect to the gauge coupling.

- A study analogous to the one of this paper in the four-dimensional case is both feasible and desirable. We expect that many of the details will be different—this is clear already from the fact that in four dimensions the need for neutral massless “spectator” fermions, dictated by two-dimensional Lorentz invariance, does not arise. We note in this regard the study of [28], showing, within an analytic strong-coupling expansion the existence of a strong-coupling symmetric phase in a four-dimensional Yukawa-Higgs model with GW fermions (this result is backed-up by Monte Carlo simulations [29]).

2 The proposal

In this section, we review the proposal of [12]. It has many desirable features:

- It is a full lattice proposal for a local action and measure for a chiral gauge theory.
- The realization of both anomalous and anomaly-free global symmetries is exactly as in the target continuum theory.
- Arguments in support of the conjecture that at strong Yukawa coupling the theory is in a symmetric phase with a chiral massless spectrum were given in ref. [12].

We believe that the three points above warrant the further study of the proposal. In this paper, we investigate the properties of this “Yukawa-Higgs-GW-fermion” lattice model in more detail. First, we repeat the formulation of the model [12]. Then, we subject the third point above to a detailed analysis.

2.1 The continuum “345” model and its symmetries

We will present the proposal on the example of a two-dimensional $U(1)$ chiral gauge theory. The condition for a two-dimensional $U(1)$ gauge theory to be free of gauge anomalies is that the sum of the squares of the charges of the left and right handed modes must cancel $\sum_i q_{i,left}^2 - \sum_j q_{j,right}^2 = 0$. An example of such a theory is the “345” theory where there are left-handed fermions of charge 3 and 4 and right-handed fermions of charge 5, so the chiral fermion spectrum is simply denoted as $3_-, 4_-, 5_+$. The model is asymptotically free and can be solved via bosonization (its spectrum was found in [30]).

The “345” $U(1)$ theory has two anomaly free global symmetries, the “133” symmetry (in a notation where 3_- has charge 1, and 4_- and 5_+ —charge 3), and the global part of the “345” gauge symmetry. The fermion number “111” symmetry has an anomaly and the associated ’t Hooft operator is, schematically, of the form $(3_-)^3 \partial_+ (4_-)^4 (\bar{5}_+)^5$.

2.2 GW kinetic terms and exact chiral symmetries

To begin describing the proposal, we introduce three two-dimensional Dirac fermions, Ψ_3, Ψ_4, Ψ_5 , charged under the $U(1)$ gauge group with charges 3, 4, 5, respectively. There is also a neutral Dirac

fermion, Ψ_0 . The fermion fields live on the sites, labeled by $\{x\}$, of a two dimensional lattice and their lattice action consists of kinetic terms:

$$S_{kin} = \sum_{q=0,3,4,5} \sum_{x,y} \bar{\Psi}_q D_{q,x,y} \Psi_{q,y} , \quad (2.1)$$

where D_q is the Neuberger operator for a fermion of charge q , obeying the GW relation:⁵

$$\{D_q, \gamma_5\} = D_q \gamma_5 D_q . \quad (2.2)$$

Here γ_5 is the appropriate two-dimensional matrix and the lattice spacing has been set, from now on, to unity. The lattice action (2.1) has a large number of exact global symmetries:

$$\prod_{q=0,3,4,5} U(1)_{q,-} \times U(1)_{q,+} , \quad (2.3)$$

where $U(1)_{q,\pm}$ acts only on the Dirac fermion field of charge q :

$$\Psi_q \rightarrow e^{i\alpha_{q,\pm} P_{\pm}} \Psi_q , \quad \bar{\Psi}_q \rightarrow \bar{\Psi}_q e^{-i\alpha_{q,\pm} \hat{P}_{\mp}} , \quad (2.4)$$

where $P_{\pm} = (1 \pm \gamma_5)/2$ and $\hat{P}_{\pm} = (1 \pm \hat{\gamma}_5)/2$, with $\hat{\gamma}_5 \equiv (1 - D)\gamma_5$. That $\hat{\gamma}_5^2 = 1$ follows from the GW relation (2.2); note that Ψ_q and $\bar{\Psi}_q$ transform differently, which is perfectly natural in Euclidean space. The projector used for every Ψ_q involves the appropriate Neuberger operator D_q .

That the symmetries in equation (2.4) are all exact symmetries of the action (2.1) follows from $\hat{P}_{\mp} D = D P_{\pm}$, yet another consequence of the GW relation (2.2). The measure of integration, however, is not invariant under any individual $U(1)_{q,+}$ or $U(1)_{q,-}$. Instead, under an infinitesimal $U(1)_{q,\pm}$ transformation (2.4) with parameter $\alpha_{q,\pm}$, the measure changes as follows:

$$U(1)_{q,\pm} : \prod_{r=0,3,4,5} d\bar{\Psi}_r d\Psi_r \rightarrow \prod_{r=0,3,4,5} d\bar{\Psi}_r d\Psi_r \left[1 - i\alpha_{q,\pm} \text{Tr} (P_{\pm} - \hat{P}_{\mp}) \right] = \prod_{r=0,3,4,5} d\bar{\Psi}_r d\Psi_r \left[1 \pm i\alpha_{q,\mp} \frac{1}{2} \text{Tr} D_q \gamma_5 \right] . \quad (2.5)$$

Eqn. (2.5) implies that for vectorlike symmetries $U(1)_{qV}$ ($\alpha_{q,+} = \alpha_{q,-}$), there is no Jacobian and thus they are true symmetries of the theory. On the other hand [5,31], since $-\frac{1}{2} \text{Tr} D_q \gamma_5 = n_+^0 - n_-^0$, the difference between the number of left- and right-handed zero modes of D_q , the continuum violation of charge for anomalous symmetries is reproduced by the nonzero Jacobian.

2.3 Reduction of the global chiral symmetries by GW-Yukawa couplings

To construct our candidate “345” chiral lattice theory, we introduce a unitary higgs field, ϕ_x , living on the lattice sites. We will use ϕ_x to write all possible Dirac and Majorana Yukawa terms that violate all symmetries (2.3) of the kinetic term (2.1) except:

$$U(1)_{3,-} \times U(1)_{4,-} \times U(1)_{5,+} \times U(1)_{0,+} . \quad (2.6)$$

⁵For a review of the GW relation and exact chiral symmetry on the lattice, see, for example, [8] and references therein.

To this end, we relate the Dirac fields Ψ_q to their chiral components: $\Psi_{q,\pm} \equiv P_{\pm} \Psi_q$, $\bar{\Psi}_{q,\pm} \equiv \bar{\Psi}_q \hat{P}_{\mp}$; note that the definition of the $\bar{\Psi}_{\pm}$ chiral modes is now both momentum and gauge-background dependent. We then write down the most general Dirac and Majorana couplings—expected to give mass of order the inverse cutoff—to the fields:

$$\begin{aligned} X_+ &= (\Psi_{3,+}^T \bar{\Psi}_{3,+} \Psi_{4,+}^T \bar{\Psi}_{4,+}) \\ Y_- &= \begin{pmatrix} \Psi_{5,-} \\ \bar{\Psi}_{5,-}^T \\ \Psi_{0,-} \\ \bar{\Psi}_{0,-}^T \end{pmatrix}, \end{aligned} \quad (2.7)$$

where T denotes transposition (we treat unbarred Dirac spinors as columns and barred ones as rows) of the form:⁶

$$S_{mass} = y \sum_x X_{+x} M(\phi_x, \phi_x^*) Y_{-x}. \quad (2.8)$$

Both Dirac and Majorana masses are to be included for the mirror fields: if Majorana masses are omitted, there will be extra unbroken chiral symmetries and unlifted zero modes in an instanton background, resulting in failure to reproduce the 't Hooft vertex. Therefore, Majorana masses are needed in order to introduce a violation of fermion number into the lattice, as has already been noted in [32].

Instead of writing explicitly the entire matrix $M(\phi_x, \phi_x^*)$, which depends on powers of ϕ and ϕ^* determined by gauge invariance, as indicated in (2.8), we give an example of a Dirac mass term: $\bar{\Psi}_{0,-}(\phi^*)^3 \Psi_{3,+} + \bar{\Psi}_{3,+} \phi^3 \Psi_{0,-}$, and of a Majorana mass of the form: $\bar{\Psi}_{5,-} \gamma_2 \phi^8 (\bar{\Psi}_{3,+})^T - \Psi_{3,+}^T \gamma_2 (\phi^*)^8 \Psi_{5,-}$. Here γ_2 is the hermitean gamma matrix that appears when Majorana masses are written using Dirac spinors, while ϕ is the unitary Higgs field. Thus, the explicit form of $M(\phi_x, \phi_x^*)$ in (2.8) contains appropriate powers of ϕ and γ_2 -insertions. The general mass matrix (2.8) violates all $U(1)$ symmetries except the desired $U(1)_{3,-} \times U(1)_{4,-} \times U(1)_{5,+} \times U(1)_{0,+}$ symmetry from (2.6).

We continue by noting that not all symmetries (2.6) of the lattice action (2.8), (2.1) are respected by the lattice path integral measure. The measure is only invariant under three symmetries: the $U(1)_{345}$ and the $U(1)_{133}$ chiral symmetries—linear combinations of $U(1)_{3,-} \times U(1)_{4,-} \times U(1)_{5,+}$ with coefficients 345 and 133, respectively—and the $U(1)_{0,+}$, which acts only on the $n_+ \equiv P_+ \Psi_0$ neutral field, whose dynamics is expected to decouple from the physics of the charged sector. The third linear combination of the first three $U(1)$'s in equation (2.6)—the fermion number symmetry of the light charged fields, which can be taken to be the “111” symmetry—has an anomaly exactly reproduced by the Jacobian, eqn. (2.5), of the corresponding transformation of the measure; see [5], [31], and references in [8]. Thus, the lattice theory obeys exact Ward identities, including the anomalous ones. For example, using (2.5) one finds that the 111 transform of an operator \mathcal{O} obeys the exact lattice Ward identity:

$$\langle \delta_{\alpha_{111}} \mathcal{O} \rangle = i \frac{\alpha}{2} \langle \mathcal{O} \text{Tr} [\gamma_5 (D_3 + D_4 - D_5)] \rangle. \quad (2.9)$$

The continuum limit expansion $\text{Tr} \gamma_5 D_q \sim \int d^2x \epsilon^{\mu\nu} F_{\mu\nu}$ [31] implies that the anomalous Ward identity (2.9) has the expected continuum limit.

⁶The presence of neutral mirrors is necessary to preserve two dimensional Lorentz invariance.

At the end of this section, it is worth noting that this proposal carries some of the flavor⁷ of an earlier construction of Eichten and Preskill [13], attempting to use strong four-Fermi interactions to decouple mirrors and doublers (it is clear that integrating out our short-ranged ϕ_x will produce strong multi-fermion interactions of the mirrors). Their proposal is known not to give rise to a chiral gauge theory (see [34], where the similarity with Yukawa models was also used). In our case, the modified lattice chiral symmetry that leads to exact decoupling of the chirality components only allows us to make use of the Yukawa analogue of the strong four-Fermi coupling symmetric phase (see the Appendix of [13])—a phase with unbroken gauge symmetry, where all fermions that participate in the strong interactions are massive.

2.4 Action, partition function, and dynamics

To ensure that the dynamics of our lattice model reproduces that of the desired unbroken chiral gauge theory, we need to demonstrate the existence of a strong-Yukawa-coupling symmetric phase with chiral spectrum of massless fermions (recall again the strong coupling analysis of [22] which showed that in the waveguide model the spectrum in this phase was vectorlike). Remarkably, as we will find below, to leading order in the strong Yukawa coupling expansion and small gauge coupling—precisely the regime where the waveguide idea broke down—there appear no new massless modes and the spectrum of the unbroken gauge theory is chiral.

The total action of the lattice model is, finally:

$$S = S_{Wilson} + S_{kin} + S_{mass} + S_{\kappa} , \quad (2.10)$$

S_{kin} is defined in (2.1), S_{mass} —in (2.8), S_{Wilson} is the usual plaquette action for the link variables $U_{x,x+\hat{\mu}}$, appropriately modified to restrict the gauge field path integral to admissible gauge field backgrounds, see [8], and S_{κ} is the action for the charge-1 unitary Higgs field:

$$S_{\kappa} = \frac{\kappa}{2} \sum_x \sum_{\hat{\mu}} [2 - (\phi_x^* U_{x,x+\hat{\mu}} \phi_{x+\hat{\mu}} + \text{h.c.})] . \quad (2.11)$$

The dynamical issue that needs to be addressed is the existence of an “unbroken” phase where ϕ is disordered (analogous to $\langle \phi \rangle = 0$, versus $\langle \phi \rangle \neq 0$, in four dimensions), such that the gauge boson is massless.

In the case without fermions, it is well known [35] that theories with unitary Higgs fields (contrary to “everyday” continuum intuition) exhibit a symmetric phase, for small enough κ . The essential idea⁸ is that for small κ large fluctuations of the unitary Higgs field—or, in the equivalent unitary gauge, the pure-gauge fluctuations of the gauge field U —are not suppressed by the action (2.11) and hence their correlation length is of order the lattice spacing. Thus, integrating out the rapidly fluctuating Higgs fields results in renormalization of the gauge coupling plus a tower of higher-dimensional gauge invariant local operators which are irrelevant for the long-distance physics of the gauge theory. This is most easily seen upon integrating over the rapid fluctuations of ϕ_x , or equivalently, the pure-gauge part of U , by explicitly performing the strong-coupling (small κ) expansion. The leading correction is a small, $\mathcal{O}(\kappa^4)$, shift to the inverse gauge coupling constant,

⁷We thank David B. Kaplan for pointing this out to us. We also note that a proposal to decouple the mirrors by combining the (approximate) lattice chirality of domain wall fermions with the Eichten-Preskill ideas was made earlier in [33].

⁸Sometimes called the “FNN mechanism” [36].

$g^{-2} \rightarrow g^{-2} + \kappa^4$ (see section II.C.(a) of [35]), while the tower of higher-dimensional gauge-field dependent operators is suppressed by increasing powers of the small correlation length of ϕ_x .

Since the gauge theory (2.10) is asymptotically free, to study the continuum limit it is sufficient to begin at leading order in the $g \rightarrow 0$ expansion; here we will confine our analysis to this limit. The limit freezes the gauge degrees of freedom to $U = 1$; see also discussion in Section 3.2. The resulting theory is a unitary Higgs-Yukawa model, equivalent to the XY model coupled to fermions, whose phase structure can be studied in various limits. We are interested in the symmetric phase of the lattice XY model and will study $\kappa < \kappa_c$ while also taking $y \rightarrow \infty$ (cf. eqn. (2.8)).

In a trivial gauge background, the lattice partition function of the model (2.10) factorizes into a product $Z = Z_{light} \times Z_{mirror}$, with:

$$\begin{aligned} Z_{light} &= \int \prod_x d\Psi_{3,-} d\Psi_{4,-} d\Psi_{5,+} d\Psi_{0,+} e^{-S_{kin}[\Psi^{light}]} , \\ Z_{mirror} &= \int \prod_x d\Psi_{3,+} d\Psi_{4,+} d\Psi_{5,-} d\Psi_{0,-} d\phi e^{-S_{kin}^{mirror}[\Psi^{mirror}] - S_\kappa[\phi] - S_{mass}[\Psi^{mirror}, \phi]} , \end{aligned} \quad (2.12)$$

where we used the decomposition of the Dirac fermion measure into left- and right-chirality measures, $d\Psi = d\Psi_+ d\Psi_-$, see following Sections, and, for conciseness, omitted the conjugate fields in the measure. We also denoted collectively by Ψ_{light} the fields $\Psi_{3,-}, \Psi_{4,-}, \Psi_{5,+}, \Psi_{0,+}$, and by Ψ_{mirror} the heavy charged mirrors $\Psi_{3,+}, \Psi_{4,+}, \Psi_{5,-}$, and the neutral $\Psi_{0,-}$. The “mass” term is given by equation (2.8) and the kinetic term for ϕ by (2.11).

The most important point is the splitting of the kinetic terms (2.1) into light and mirror modes in (2.12). This follows from the identity, which also holds in an arbitrary gauge background:

$$\bar{\Psi}_q D_q \Psi_q = \bar{\Psi}_{q,+} D_q \Psi_{q,+} + \bar{\Psi}_{q,-} D_q \Psi_{q,-} , \quad (2.13)$$

where the cross-terms vanish due to the GW relation (2.2). Thus the mirror and light partition functions factorize at $g = 0$. We stress that the GW relation was crucial in order for (2.13) to hold; there is no other way to achieve (2.13), and hence the factorization (2.12), on the lattice, for D_q free of doublers.

Finally, let us study Z_{mirror} and its effect on the light modes, in the $y \rightarrow \infty$ and $\kappa < \kappa_c$ limit. Of particular concern is the possible appearance of extra massless states and the associated vanishing of the mirror determinant. To this end, we redefine the mirror fermion fields in (2.12), $\Psi_{3,+}, \Psi_{4,+}, \Psi_{5,-}$, and the singlet $\Psi_{0,-}$, by $1/\sqrt{y}$. This multiplies their kinetic terms by $1/y$. Thus, as $y \rightarrow \infty$, the mirror fields kinetic terms vanish, and the mirror fermion action consists solely of a Yukawa term given by (2.8) with $y = 1$:

$$S_{mass} = \sum_x X_{+x} M(\phi_x, \phi_x^*) Y_{-x} . \quad (2.14)$$

We can now perform the integral over the mirror fermions in Z_{mirror} . The notation in the above equation might lead one to believe that the mirror fermion path integral is a product of strictly local factors:

$$\prod_x \det M(\phi_x, \phi_x^*) ,$$

where $M(\phi_x, \phi_x^*)$ is the 8×8 matrix from (2.8, 2.14), which is gauge covariant and depends only on the values of ϕ_x at x . Since ϕ_x is unitary, this would imply that the gauge invariant $\det M(\phi_x, \phi_x^*)$

is *a.*) ϕ -independent and *b.*) nonzero. Hence, we would have been led to believe that the dynamics governing the fluctuations of the pure-gauge degrees of freedom is unaffected by the mirror fermions, to leading order in $1/y$. Moreover, this argument would also imply that there is no fine-tuning, at large y , required in order to keep the XY model in its high-temperature phase. Finally, a constant determinant, as would be obtained at large- y from the above argument, indicates that there are no massless fermion states, as a massless fermion state is expected to lead to a zero determinant.

The true story, however, is more complicated than the discussion of the previous paragraph. This is due to the fact that the various $\bar{\Psi}_{\pm}$ chiral components which enter X_{+x}, Y_{-x} (2.7) and S_{mass} are somewhat smeared due to the nonlocality of the chiral projectors that define the chiral components for the barred fields. However, the extent of the nonlocality of the $\bar{\Psi}_{\pm}$ -component is small, governed by the range of nonlocality of Neuberger's operator, which is of order of the lattice spacing with an exponential tail, as the analysis of [37, 38] shows. Hence, one expects that the qualitative arguments of the previous paragraph still hold, together with the conclusion that the mirror fermion fluctuations do not significantly affect the pure gauge fluctuations and their determinant is nonzero. Section 3.3 is devoted to verifying this conjecture.

3 The simpler “toy” model

3.1 Definition of the toy model: action and symmetries

In our analytic and numerical study, we will use a simpler model that captures the main features of the mirror sector dynamics at $g = 0$. The model has a minimal field content, allowing an exhaustive study of the phase diagram using numerical methods with the computer resources available to us.

Our toy model is a $U(1)$ lattice gauge theory with one charged Dirac fermion, ψ , of charge 1, and a neutral spectator, χ . The desired spectrum of light fields in the target theory is the charged ψ_+ and the neutral χ_- . The chirality components for the charged and neutral fermions are defined, as in the previous section, by the projectors which include the appropriate Neuberger operators D_1 or D_0 for the barred components. The fermion part of the action of our toy model is:

$$\begin{aligned} S &= S_{light} + S_{mirror} \\ S_{light} &= (\bar{\psi}_+, D_1 \psi_+) + (\bar{\chi}_-, D_0 \chi_-) \\ S_{mirror} &= (\bar{\psi}_-, D_1 \psi_-) + (\bar{\chi}_+, D_0 \chi_+) \\ &\quad + y \{ (\bar{\psi}_-, \phi^* \chi_+) + (\bar{\chi}_+, \phi \psi_-) + h [(\psi_-^T, \phi \gamma_2 \chi_+) - (\bar{\chi}_+, \gamma_2 \phi^* \bar{\psi}_-^T)] \} . \end{aligned} \tag{3.15}$$

Here $\phi_x = e^{i\eta_x}$ is the unitary higgs field and we do not show its kinetic term as it is the same as in (2.10). The brackets indicate both summation over coordinates and an inner product of spinors, for example $(\bar{\psi}_-, \phi^* \chi_+) \equiv \sum_x \bar{\psi}_{-x} \phi_x^* \chi_{+x}$ and $(\bar{\psi}_+, D_1 \psi_+) \equiv \sum_{x,y} \bar{\psi}_{+x} D_{1xy} \psi_{+y}$. There are two Yukawa couplings in the model, y and yh , which are both taken real. The coupling h measures the ratio of the Majorana to Dirac mass, while y is the overall strength of the Yukawa coupling. The S_{mirror} term above is the analogue of (2.8) in the “345” theory.

When $y = h = 0$, the lattice action (3.15) has four global $U(1)$ symmetries, as every chiral component can be rotated independently, as in Section 2. When both y and h are nonzero, there are only two $U(1)$ symmetries, acting on ψ_+ and χ_- , respectively. The first is the anomalous global part of the gauge group and the second is the global symmetry of the spectator fermion. When $h = 0$, the Majorana mass vanishes, and we have one extra exact $U(1)$ that also acts on the charged

fields and leads to extra zero modes. Hence, we also need $h \neq 0$, as we will explicitly see below; note that the phase diagram for a four-dimensional model very similar to ours, without Majorana mass terms has recently been considered in [28], using analytical methods.⁹

The continuum target theory that (3.15) is conjectured to flow to is the chiral Schwinger model, an anomalous $U(1)$ gauge theory with a single right-handed massless fermion of unit charge (ψ_+), a model solved in [30, 39]. Since our paper is confined to the study of only the mirror fermion-Higgs dynamics, without gauge fields and without taking massless fermion loops into account, we do not have to cancel anomalies of the light spectrum; minimality of the field content is why the “toy” model was chosen as an arena to study the strong mirror-sector dynamics.

The fermion action (3.15), the gauge action, and S_κ (the action of ϕ in (2.11)), combined with the usual Dirac fermion measure and the measures for the $U(1)$ link fields and ϕ_x , completely define the lattice partition function of the toy model. As a matter of principle, the lattice model defined above could be, right away, subjected to numerical simulations including both dynamical gauge fields and fermions. However, this is beyond the scope of this paper, which is restricted to the $g = 0$ case. Clearly, this is only a first relatively simple step in the full analysis of the dynamics and the utility of the proposal. Working out the dynamics at $g = 0$ is also a litmus test for the proposal: if the analysis fails to yield a chiral spectrum or an unbroken gauge symmetry (more precisely—its global counterpart) at this point, the proposal has to be abandoned and no further study at $g \neq 0$ is warranted.

3.2 The toy model partition function at $g = 0$

When $g \rightarrow 0$, only zero-action fluctuations of the gauge field contribute to the path integral. In other words, $U_{x,y} = \omega_x \omega_y^\dagger$ with $\omega_x = e^{i\alpha_x}$. The ω_x fields appear in the kinetic terms of (3.15) and in the Yukawa couplings, via the projectors used to define chirality components $\bar{\psi}_\pm$ of the charged $\bar{\psi}$. We can remove the ω_x dependence in the lagrangian by a local field redefinition of $\bar{\psi}$, ψ , and ϕ :

$$\psi_x = e^{i\alpha_x} \psi'_x, \quad \bar{\psi}_x = \bar{\psi}'_x e^{-i\alpha_x}, \quad \phi_x = e^{-i\alpha_x} \phi'_x, \quad (3.16)$$

with unit Jacobian. Thus the path integral over the ω_x decouples, yielding the volume of the group. We are left, dropping the primes, with a nontrivial integral over ψ , χ , and ϕ .

Now, as explained in Section 2, the partition function in a trivial gauge background splits into a product of mirror and light partition functions. As also explained there, for the purpose of the study of the $g = 0$ dynamics of the mirror fermion sector, the chiral split of the measure should be worked out explicitly, in order to make the decoupling of the light and mirror sector manifest and to facilitate a Monte Carlo study of the mirror sector dynamics.

To work out the \pm -chirality split, it is useful to define the measure in terms of eigenvectors of the Neuberger operator. Since the chiral projectors involve the Neuberger operator, using its eigenvectors to define the measure facilitates an easy split of the measure into chiral components. The details are straightforward but somewhat tedious and are given in Appendix A. For the reader interested in the final formulae, the important expressions are eqn. (A.30)—the expansion of the GW-chirality components of spinors in terms of GW momentum eigenstates—and eqn. (A.17), the final form of the measure relevant for its chiral split (also reproduced here in (3.19), (3.20)). In

⁹We also need $h \neq 1$: at $h = 1$ the mirror fermion spectrum has an exact zero mode at finite N for arbitrary ϕ_x backgrounds, see Section 3.2.

this section, we only present the final expression for the partition function and measure resulting from applying these formulae.

We start with the partition function written in terms of position space variables, the charged $\{\psi_{\pm x}, \bar{\psi}_{\pm x}\}$ and neutral $\{\chi_{\pm x}, \bar{\chi}_{\pm x}\}$, in terms of which the chiral split of the measure is quite complicated. Then, we change variables, using (A.30), in both the action and measure in terms of appropriately chosen—corresponding to the GW eigenvalues with positive imaginary part—momentum space variables $\{\psi_{\pm x}, \bar{\psi}_{\pm x}\} \rightarrow \{\alpha_{\mathbf{k}\pm}, \bar{\alpha}_{\mathbf{k}\pm}\}$ and $\{\chi_{\pm x}, \bar{\chi}_{\pm x}\} \rightarrow \{\beta_{\mathbf{k}\pm}, \bar{\beta}_{\mathbf{k}\pm}\}$. After performing all the required summations over x, y , the results for the various components of S_{light} and S_{mirror} are as described below.

The kinetic terms for the mirror and light fermions from (3.15) become, see (A.13):

$$S_{mirror}^{kin} = \sum_{\mathbf{k}} \lambda_{\mathbf{k}} (\bar{\alpha}_{\mathbf{k}-} \alpha_{\mathbf{k}-} + \bar{\beta}_{\mathbf{k}+} \beta_{\mathbf{k}+}) , \quad (3.17)$$

$$S_{light}^{kin} = \sum_{\mathbf{k}} \lambda_{\mathbf{k}} (\bar{\alpha}_{\mathbf{k}+} \alpha_{\mathbf{k}+} + \bar{\beta}_{\mathbf{k}-} \beta_{\mathbf{k}-}) . \quad (3.18)$$

Here $\lambda_{\mathbf{k}}$ is the eigenvalue of the free Neuberger operator with positive imaginary part, eqn. (A.22), corresponding to momentum \mathbf{k} . The most important properties of $\lambda_{\mathbf{k}}$ are that $\lambda_{\mathbf{k}} - 1$ is a complex number of unit modulus, a consequence of the GW condition, and that $\lambda_{\mathbf{k}}$ only has a zero at $\mathbf{k} = \mathbf{0}$, see (A.22). The momentum sums here and below are over $k_1, k_2 = 1, \dots, N$.

The measure of the $g = 0$ partition function, see eqn. (A.17), splits naturally into a measure for the light fermions $\alpha_{\mathbf{k}+}, \bar{\alpha}_{\mathbf{k}+}, \beta_{\mathbf{k}-}, \bar{\beta}_{\mathbf{k}-}$:

$$\prod_x d\bar{\psi}_{+x} d\psi_{+x} d\bar{\chi}_{-x} d\chi_{-x} \equiv \prod_{k_1, k_2=1}^N 16(1 - \lambda_{\mathbf{k}}^*) d\alpha_{\mathbf{k}+} d\bar{\alpha}_{\mathbf{k}+} d\beta_{\mathbf{k}-} d\bar{\beta}_{\mathbf{k}-} , \quad (3.19)$$

and a measure for the mirror fermions $\alpha_{\mathbf{k}-}, \bar{\alpha}_{\mathbf{k}-}, \beta_{\mathbf{k}+}, \bar{\beta}_{\mathbf{k}+}$:

$$\prod_x d\bar{\psi}_{-x} d\psi_{-x} d\bar{\chi}_{+x} d\chi_{+x} \equiv \prod_{k_1, k_2=1}^N 16(1 - \lambda_{\mathbf{k}}^*) d\alpha_{\mathbf{k}-} d\bar{\alpha}_{\mathbf{k}-} d\beta_{\mathbf{k}+} d\bar{\beta}_{\mathbf{k}+} . \quad (3.20)$$

To complete the definition of the mirror fermion partition function Z_{mirror} , we need to write the Yukawa couplings of the mirror fermions in S_{mirror} (3.15) to the unitary Higgs field. To this end, we first define the Fourier transforms of $\phi_x = e^{i\eta_x}$, with $\omega_N \equiv e^{\frac{2\pi i}{N}}$:

$$\Phi_{\mathbf{k}} \equiv \frac{1}{N^2} \sum_{\mathbf{x}} \omega_N^{-\mathbf{k} \cdot \mathbf{x}} e^{i\eta_x} , \quad \Phi_{\mathbf{k}}^* \equiv \frac{1}{N^2} \sum_{\mathbf{x}} \omega_N^{-\mathbf{k} \cdot \mathbf{x}} e^{-i\eta_x} = (\Phi_{-\mathbf{k}})^* . \quad (3.21)$$

The two Yukawa couplings in the toy model lagrangian are, then:

$$\begin{aligned} \frac{1}{y} S_{mirror}^{Dirac} &= \frac{1}{2} \sum_{\mathbf{k}, \mathbf{p}} (2 - \lambda_{\mathbf{k}}) \left(\bar{\alpha}_{\mathbf{k}-} \beta_{\mathbf{p}+} \Phi_{\mathbf{k}-\mathbf{p}}^* + \bar{\beta}_{\mathbf{k}+} \alpha_{\mathbf{p}-} \Phi_{\mathbf{k}-\mathbf{p}} e^{i(\varphi_{\mathbf{p}} - \varphi_{\mathbf{k}})} \right) , \\ \frac{1}{yh} S_{mirror}^{Maj} &= \end{aligned} \quad (3.22)$$

$$i \sum_{\mathbf{k}, \mathbf{p}} \left[\alpha_{\mathbf{k}-} \beta_{\mathbf{p}+} \Phi_{-\mathbf{k}-\mathbf{p}} e^{i\varphi_{\mathbf{k}}} - \bar{\beta}_{\mathbf{k}+} \bar{\alpha}_{\mathbf{p}-} \Phi_{\mathbf{k}+\mathbf{p}}^* \frac{(2 - \lambda_{\mathbf{p}})(2 - \lambda_{\mathbf{k}}) e^{-i\varphi_{\mathbf{k}}} - \lambda_{\mathbf{p}} \lambda_{\mathbf{k}} e^{-i\varphi_{\mathbf{p}}}}{4} \right],$$

where the momentum-dependent phase factors $e^{i\varphi_{\mathbf{k}}}$ are defined in eqn. (A.28).

The existence of an exact mirror-fermion zero mode at $h = 1$, alluded to in Section 3.1 and evident in all our numerical results, for arbitrary ϕ_x backgrounds, can now be shown. The mirror zero mode at $h = 1$ is a Majorana-Weyl fermion: this can be seen by letting all but the $\mathbf{k} = 0$ components of $\beta_{\mathbf{k}+}, \bar{\beta}_{\mathbf{k}+}$ vanish, taking $\beta_{\mathbf{0}+} = -i\bar{\beta}_{\mathbf{0}+}$, and showing that the mirror action (3.22) vanishes if $h = 1$.

The equations presented in this section completely define the partition function. The decoupling of the light and mirror partition functions is manifest. The mirror partition function Z_{mirror} is defined by means of the fermion measure (3.20), the measure for the unitary Higgs field, $\prod_x \int_0^{2\pi} d\eta_x$, and the action $S_{mirror} = S_{mirror}^{kin} + S_{mirror}^{Dir} + S_{mirror}^{Maj} + S_{\kappa}$, with the various terms defined in (3.17), (3.22), and (2.11).

As mentioned in the Introduction, the split of the measures allows us, from now on, to concentrate on studying the properties of the mirror fermion-Higgs sector with partition function Z_{mirror} .

3.3 Evidence for the existence of a symmetric phase at strong Yukawa coupling

In this Section, we present our study of the symmetry realization in the mirror theory at strong Yukawa coupling. We remind the reader that the two possibilities are:

1. A disordered (“symmetric”) phase, where correlation lengths are of order the lattice spacing. The absence of order in the Higgs field is the analogue of the symmetric phase in four dimensions. The gauge boson would remain massless, apart from the mass generated by the Schwinger mechanism.
2. A quasi-ordered phase, where correlations fall off according to a power law. In this phase the gauge boson would acquire a mass-squared of order κg^2 . It is the two-dimensional analogue of spontaneous gauge symmetry breaking in four dimensions.

In the quasi-ordered phase there are long wavelength modes that could mix with fermion bilinear composites and form light mirror sector states. Hence any indication of critical behavior in susceptibility data will be a sign of possible problems for the decoupling of the mirror sector. To this end, we perform a Monte Carlo simulation of the mirror theory, whose partition function was defined in Section 3.2; all averages are computed using the Monte Carlo techniques described in Appendix C.

Apart from a few remarks below, all simulations are done in the limit when the kinetic term of the mirror fermions, eqn. (3.17), is neglected, i.e. in the strong Yukawa coupling limit $y \rightarrow \infty$ (cf. Appendix C.1). The ratio of Majorana to Dirac Yukawa couplings, the parameter h in (3.22), is kept fixed. For $N = 4, 8, 16$, our results indicate that in this limit:

- There is no sign problem for the fermion determinant at $h > 1$. We have no analytic proof for arbitrary ϕ_x background (we have been able to show positivity for a constant background and to first order in small fluctuations). However, based on our simulations of the determinant in many (tens of millions) arbitrary ϕ backgrounds, not a single configuration has lead to a negative determinant for $h > 1$. The results of the simulations and the presence of the exact zero mode at $h = 1$ suggest that it should be possible to find an analytic proof of positivity.

- For $0 < h < 1$ there is a sign problem and indications of critical behavior, as described below.
- All correlation lengths, for $\kappa = 0.1, 0.5$ (both smaller than the XY -model $\kappa_c \simeq 1.12$) are $\mathcal{O}(a)$ and there is no critical behavior for $h > 1$ as discussed below.
- Within errors, for all $h > 0$, there is no direction of η that is favored. The shift symmetry $\eta \rightarrow \eta + \text{const.}$ seems to be preserved. However, this is not a test of quasi-order, as we need to look at the response to a small external perturbation—hence, we perform the susceptibility measurements.
- The susceptibility, for the same values of κ , shows a large response for $h < 1$ that increases with volume, indicative of quasi-order, and a small response for $h > 1$, indicative of the absence of quasi-ordering.
- The vortex density decreases as h decreases towards $h = 1$, as in the Berezinski-Kosterlitz-Thouless transition towards the low-temperature “confined-vortex” phase.

In this summary, and in the discussion that follows, it is important to keep in mind that the phase transition at $h = 1$ is not sharp at finite N . Therefore when we speak of properties at, say, $h > 1$, what is implied is behavior at $h > 1 + \epsilon$ with $\epsilon > 0$ a small number that tends to zero as $N \rightarrow \infty$.

3.3.1 Scalar field susceptibility

We begin with a study of the scalar field susceptibility, which is a measure of the long distance correlations of the XY -model field $\phi_x = e^{i\eta_x}$. In the “high-temperature” disordered phase of the XY model the susceptibility is small, of order the lattice spacing or less, depending on the value of $\kappa < \kappa_c$. The critical coupling for the pure XY model on a square lattice is known to be $\kappa_c \sim 1.12$ [40]. In the “low-temperature” phase with algebraic long-range order, the susceptibility increases with the volume of the system.

The susceptibility, which can also be thought of as the zero-momentum propagator of ϕ_x , is defined in the usual way:

$$\chi = \frac{1}{N^2} \left\langle \left| \sum_x e^{i\eta_x} \right|^2 \right\rangle. \quad (3.23)$$

For an explanation of the meaning and numerical implementation of the $\langle \dots \rangle$ average, see Appendix C.

We now present the results of numerical simulations of the scalar field susceptibility (3.23). First, in Fig. 1, we show the susceptibility for $\kappa = 0.1$ for $N = 4, 8, 16$, as a function of h ; the pure XY -model values are shown by horizontal dashed lines. We see that for $h > 1$ the fermions do not have an appreciable effect on the scalar field susceptibility. Similar results are obtained for $\kappa = 0.5$, with the resulting overall rise in susceptibility, due to the closeness of κ to $\kappa_c = 1.12$, and are shown on Fig. 2. Finally, in Fig. 3, we give the result for $\kappa = 0$. It is qualitatively similar to the $\kappa = 0.1, 0.5$ results.

The results of the simulations of the scalar susceptibility displayed here show that for $h > 1$ the fermions have a negligible effect on the scalar field susceptibility. The results of this Section

h	N	χ	N	χ	N	χ
0.01	4	3.15(7)	8	3.42(16)	16	3.42(14)
0.005	4	3.15(6)	8	3.41(16)	16	3.41(14)
0.001	4	3.14(7)	8	3.41(16)	16	3.40(14)

Table 1: $\kappa = 0.1$ results for small values $h \rightarrow 0$; note that no $h \rightarrow 0$ extrapolation is required, as the limit is already obtained within error and the susceptibility χ appears to approach a constant value as $N \rightarrow \infty$.

support the conjecture that at strong Yukawa coupling the theory remains in the symmetric phase. We also note that the susceptibility of the theory with fermions, for $h > 1$, is somewhat lower than the susceptibility of the pure XY -model with the same value of κ , for $N \gg 1$. This can be interpreted as a small renormalization of κ to smaller values due to the fermions, which appear to push the theory further into the symmetric phase.

On the other hand, for $h \leq 1$, there are indications of critical behavior and the scalar susceptibility grows with the volume of the system, as appropriate for the low-temperature phase of the XY model. Also, for $h \simeq 1$, the fermion determinant vanishes and there is a massless mirror fermion state (see the footnote in Section 3.1 and the numerical analysis of the spectrum in Section 3.4). Clearly, at these values of h , the sensitivity to $y < \infty$ is enhanced, see Section C.1 in the Appendix C.

Finally, for $h \rightarrow 0$, in Table 1 we show the $\kappa = 0.1$ results for the Higgs susceptibility. Clearly there is a finite $h \rightarrow 0$, $N \rightarrow \infty$ limit, contrary to the finite-size scaling that would occur in a quasi-ordered phase. We conclude that the Higgs is in the disordered phase also for $h = 0$, in agreement with the analytic [28] and numerical [29] results in a similar model ($h = 0$) in four dimensions.

3.3.2 Binder cumulant

The Binder cumulant [24] is a quantity probing higher-order correlations, defined as:

$$U = 2 - \frac{\langle |M|^4 \rangle}{\langle |M|^2 \rangle^2}, \quad (3.24)$$

where M is the total “magnetization:” $M = \sum_x \phi_x$, $|M|^2 \equiv MM^*$, $|M|^4 \equiv (|M|^2)^2$. The definition (3.24) is chosen such that in the pure XY -model U interpolates between 0 and 1 as the temperature decreases from infinity to zero:

$$\lim_{\kappa \rightarrow 0} U = 0, \quad \lim_{\kappa \rightarrow \infty} U = 1. \quad (3.25)$$

This is easily seen by noting that for $\kappa = 0$, there is no intersite correlation and hence U can be computed by treating the ϕ_x as random, delta-correlated, field leading to $U = 0$. On the other hand, for $\kappa = \infty$, there is perfect order in each configuration and the ϕ_x are frozen, giving rise to $U = 1$.

We show the results of the measurement of the Binder cumulant for two values of κ : $\kappa = 0.1$ in Fig. 4 and $\kappa = 0.5$ in Fig. 5. In each case, as a function of h the Binder cumulant behaves as if $h \leq 1$ corresponds to the broken phase of the XY model and $h > 1$ —to the unbroken phase, consistent with the measurement of the scalar susceptibilities of the previous section, and thus providing further evidence for the persistence of the symmetric phase at strong Yukawa coupling and $h > 1$.

3.3.3 Vortex density

The Berezinski-Kosterlitz-Thouless transition in the XY -model can be interpreted, see [23], as due to the deconfinement of vortices above the critical temperature (at $\kappa \leq \kappa_c$). The definition and algorithm of finding the vortex density—the number of vortex-antivortex pairs per XY spin—is described in [41].

We studied the vortex density as a function of h . We show the results, for $\kappa = 0.5$, on Fig. 6. It is clear from the figure that the vortex density of the deformed XY model at $h > 1$ is slightly higher than the value appropriate to the pure- XY model for $\kappa = 0.5$; this is consistent with the susceptibility measurements, where the small effect of the fermions at large y is to push the theory further into the symmetric phase.

To summarize, in Sections 3.3.1, 3.3.2, and 3.3.3, we presented measurements of the pure scalar probes of symmetry breaking—the scalar susceptibility, the Binder cumulant, and the vortex density. The results give strong support in favor of the existence of a symmetric phase at strong Yukawa coupling, at $h > 1$, $\kappa < 1$.

3.3.4 Fermion bilinear susceptibilities

In this Section, we consider another probe of symmetry breaking—the fermion susceptibilities. As discussed in the Introduction, a scalar ϕ_x and a charged mirror fermion, ψ_- , can produce a neutral fermion bound state at strong coupling. Similarly, one expects that a charged and a neutral fermion, ψ_- and χ_+ , can bind into scalar bound states with the quantum numbers of ϕ_x .

The two composite charged complex scalars of lowest dimension that we can construct out of bilinears of the mirror fermions are $\bar{\psi}_- \chi_+$ and $\psi_-^T \gamma_2 \chi_+$. We then define the corresponding susceptibilities; similar to the scalar case (3.23) they can be interpreted as the zero-momentum propagators of the corresponding composite scalar fields. Thus, we introduce the “Dirac” susceptibility:

$$\chi_F \equiv \sum_x \langle \bar{\psi}_- x \chi_+ x \bar{\chi}_+ y \psi_- y \rangle, \quad (3.26)$$

and the “Majorana” susceptibility:

$$\chi'_F \equiv \sum_x \langle \psi_-^T x \gamma_2 \chi_+ x \bar{\chi}_+ y \gamma_2 \bar{\psi}_-^T y \rangle. \quad (3.27)$$

In four dimensions a disconnected part would also have to be subtracted; however, the disconnected part always vanishes in two dimensions due to the absence of spontaneous symmetry breaking. The explicit form of χ_F and χ'_F in terms of averages over the variables of integration introduced in Section 3.2 is given in eqns. (B.16, B.19) of Appendix B. Note that the dimensionless fermion susceptibilities scale as Y^{-2} , at large dimensionless $Y \equiv ya$.

The results for the modulus and argument of the Dirac susceptibilities are given, for $\kappa = 0.5$ in Figs. 7 and 9, respectively. Similarly, for the Majorana susceptibility, the results for $\kappa = 0.5$ are shown in Figs. 12 and 13, respectively. The same plots of the magnitude and arguments of the Dirac and Majorana fermion susceptibilities, this time for the smaller value of $\kappa = 0.1$ are given in Figs. 8, 10, 11, 14 and lead to the same qualitative conclusions.

We observe that the behavior of their modulus follows, as a function of h , the behavior of the scalar susceptibility and the Binder cumulant. We note the following dependence on system volume:

- For $\kappa = 0.1$ and $h > 1$, the fermion susceptibilities never show a trend of increasing with N . While the curves for $\kappa = 0.5$ are not monotonic, there we also find no evidence for finite-size scaling that would indicate the presence of light modes.
- χ'_F shows a trend of increasing for $h < 1$, for either κ . For χ_F , the trend depends on κ . This indicates that the two susceptibilities are indeed independent probes of long distance behavior. The rise in either with N is indicative of light modes that exist at $h < 1$.

The numerical results for the phases of the Dirac and Majorana susceptibilities at $h > 1$ are consistent with phases equal to 0 and π , respectively.

As a matter of comparison, we have also studied the fermion susceptibilities in the broken phase, upon increasing $\kappa > \kappa_c$. In the broken phase, the fermion susceptibilities (as well as the scalar susceptibility) show a dramatic increase with the volume of the system, which is clearly absent at $\kappa < 1$.

Overall, our results for the fermion susceptibilities show no sign of critical behavior at $h > 1$, and thus provide more evidence for the existence of a strong Yukawa symmetric phase.

3.4 Evidence for the absence of massless mirror fermions at strong Yukawa coupling

In this Section, we turn to the fermion spectrum at strong Yukawa coupling $y \gg 1$ and $\kappa < 1$. We study two kinds of correlators: those that probe the neutral fermion spectrum and those probing the charged fermion sector. All correlators that violate the $U(1)$ symmetry, i.e. of the form $\bar{\psi}_+ \chi_-$, vanish, due to the absence of spontaneous symmetry breaking of a continuous symmetry in two dimensions¹⁰ [19].

In the disordered phase the mirror fermions obtain mass by the mechanism explained in the Introduction [18], [13–17]: a charged fermion can bind with the charged scalar and pair up with the neutral fermion into a heavy neutral bound state. It is also clear that in the disordered phase, the charged mirror fermion spectrum (if charged stable single-particle states exist) is vector-like: the neutral mirror fermion can bind with the scalar into a charged right-handed fermion, which then can pair up with the charged left-handed fermion into a heavy charged state. We will study correlators that probe the spectrum of both types.

Studying the fermion propagators in the $y \rightarrow \infty$ limit will be a reliable guide to the spectrum of the mirror fermion theory at $y \gg 1$, so long as there are no massless states that invalidate the $1/y$ -expansion and make the $y < \infty$ corrections important. Further comments on the $y < \infty$ limit are given in Appendix C.1; especially important is the numerical result $\ln \text{Pf } \mathcal{M} = \ln \det M$ mentioned there. Thus, the absence of massless states for $h > 1$ that we find ensures the self-consistency of the analysis. To probe the fermion spectrum at large y , we thus study the Green functions which do not vanish in the large- y limit (note that at infinite y , all $++$ and $--$ correlators vanish).

To study the fermion spectrum of our model, we begin by first considering the charged fermions. Using ψ_- , χ_+ , and ϕ , the three simplest unit-charge local fermion operators can be defined:

$$\eta_{1x}^c = \psi_{-x} \ , \quad \eta_{2x}^c = \chi_{+x} \phi_x^* \ , \quad \eta_{3x}^c = \bar{\chi}_{+x}^T \phi_x^* \ . \quad (3.28)$$

¹⁰As a check on our numerical simulations, we have verified this property in both the disordered and quasi-ordered phases.

Negative charge fermions can, similarly, be created by the local operators:

$$\bar{\eta}_{1x}^c = \bar{\psi}_{-x}, \quad \bar{\eta}_{2x}^c = \bar{\chi}_{+x} \phi_x, \quad \bar{\eta}_{3x}^c = \chi_{+x}^T \phi_x. \quad (3.29)$$

The choice of this operator basis is motivated by simplicity and by the fact that the corresponding propagator (3.30) can also be easily computed in the quasi-ordered phase, see eqn. (B.7), and the change of the spectrum observed as a function of κ .

The propagator of the charged fermions is the connected two-point function:

$$D_{ij}^c(\mathbf{k}) = \sum_x \omega_N^{-\mathbf{k}(x-y)} \langle \eta_{ix}^c \bar{\eta}_{jy}^c \rangle, \quad i, j = 1, 2, 3. \quad (3.30)$$

Diagonalizing $D_{ij}^c(\mathbf{k})$ by a (bi-)unitary transformation gives rise to a diagonal matrix with entries, which we denote by $1/\mu_i(\mathbf{k})$ ($i = 1, 2, 3$), where the μ_i are the eigenvalues of the inverse charged fermion propagator. A massless mode would yield a zero of some of the eigenvalues μ_i for some \mathbf{k} .

The study of the spectrum is simplified at infinite y , when all $++$ and $--$ Green functions of the mirror theory vanish (there is an extra symmetry of the partition function at $y \rightarrow \infty$ forbidding such nonzero expectation values). Then it suffices to consider a reduced propagator, instead of (3.30), which we call S^c , which we obtain by keeping only the nonvanishing entries of (3.30):

$$S_{y-x}^c = \begin{pmatrix} \langle \psi_{-y} \chi_{+x}^T \phi_x \rangle & \langle \chi_{+y} \phi_y^* \bar{\psi}_{-x} \rangle \\ \langle \psi_{-y} \bar{\chi}_{+x} \phi_x \rangle & \langle \bar{\chi}_{+y} \phi_y^* \bar{\psi}_{-x} \rangle \end{pmatrix}. \quad (3.31)$$

Clearly, the propagator S^c obeys $\text{Tr} D^{c\dagger} D^c = \text{Tr} S^{c\dagger} S^c$ in the infinite- y limit. Our Monte-Carlo simulation calculates the quantity $\Omega^{(2)}(\mathbf{k})$, defined through the last equality below:

$$\text{Tr} S^{c\dagger} S^c(\mathbf{k}) = \sum_{i=1}^3 \frac{1}{|\mu_i(\mathbf{k})|^2} \equiv \left(\frac{1}{\Omega^{(2)}(\mathbf{k})} \right)^2, \quad (3.32)$$

where the Fourier transform is defined, similar to (3.30), as $S^c(\mathbf{k}) = \sum_x \omega_N^{-\mathbf{k}(y-x)} S_{y-x}^c$. Eqn. (3.32) shows that a massless particle will manifest itself as a zero of $\Omega^{(2)}$ at some \mathbf{k} . To look for light mirror modes, we will simply plot the value of $\min_{\mathbf{k}} \Omega^{(2)}(\mathbf{k})$ as a function of h and the lattice size N , for $y = \infty$.

Next, we consider the operators creating neutral mirror fermions:

$$\eta_{1x}^n = \chi_{+x}, \quad \eta_{2x}^n = \bar{\chi}_{+x}^T, \quad \eta_{3x}^n = \phi_x \psi_{-x}, \quad \eta_{4x}^n = \phi_x^* \bar{\psi}_{-x}^T, \quad (3.33)$$

with their conjugates defined as in (3.29):

$$\bar{\eta}_{1x}^n = \bar{\chi}_{+x}, \quad \bar{\eta}_{2x}^n = \chi_{+x}^T, \quad \bar{\eta}_{3x}^n = \phi_x^* \bar{\psi}_{-x}, \quad \bar{\eta}_{4x}^n = \phi_x \psi_{-x}^T, \quad (3.34)$$

and neutral fermion propagator:

$$D_{ij}^n(\mathbf{k}) = \sum_x \omega_N^{-\mathbf{k}(x-y)} \langle \eta_{ix}^n \bar{\eta}_{jy}^n \rangle, \quad i, j = 1, 2, 3, 4. \quad (3.35)$$

In the $y \rightarrow \infty$ limit it suffices to consider the reduced neutral propagator, S^n , keeping only the nonvanishing entries of (3.35) and combining them into a matrix similar to (3.31):

$$S_{y-x}^n = \begin{pmatrix} \langle \chi_{+y} \phi_x \psi_{-x}^T \rangle & \langle \chi_{+y} \phi_x^* \bar{\psi}_{-x} \rangle \\ \langle \bar{\chi}_{+y}^T \phi_x \psi_{-x}^T \rangle & \langle \bar{\chi}_{+y}^T \phi_x^* \bar{\psi}_{-x} \rangle \end{pmatrix}, \quad (3.36)$$

obeying $\text{Tr} D^{n\dagger} D^n = 2\text{Tr} S^{n\dagger} S^n$ in the infinite- y limit. We define the quantity $\Omega^{(1)}(\mathbf{k})$ by an equation identical to (3.32), but with S^c replaced with S^n ; our plots seeking to establish the presence or absence of massless neutral modes will similarly show the value of $\min_{\mathbf{k}} \Omega^{(2)}(\mathbf{k})$ as a function of h and the lattice size N , for $y = \infty$. Explicit expressions giving S^c and S^n in terms of the integration variables of Section 3.2 are given in (B.2, B.12) of Appendix B. We use the expressions given there to calculate the $\Omega^{(1),(2)}$ in our Monte-Carlo simulation.

In the broken phase, when $\phi_x \equiv 1$ to leading order in perturbation theory, the form of S^c (and S^n , which coincides with it in this limit) and the perturbative spectrum, valid when $\kappa \rightarrow \infty$, are worked out in Appendix B. An important check on our Monte Carlo simulation is that, for $\kappa \gg \kappa_c$ it reproduces the perturbative spectrum of eqns. (B.9, B.10), including all the small eigenvalues found analytically to leading order in perturbation theory, see eqn. (B.10). Furthermore, the small deviations of the Monte Carlo results from the perturbative spectrum can be seen to scale as the expected perturbative corrections to the tree-level result arising from spin-wave exchange, $\sim h^2 \kappa^{-1}$ (we find that these corrections become numerically significant for $h > 2$ for the smallest eigenvalues of $s(\mathbf{k})^{-1}$, see (B.9)).

The quantities $\min_{\mathbf{k}} \Omega_{(\mathbf{k})}^{(1)}$ and $\min_{\mathbf{k}} \Omega_{(\mathbf{k})}^{(2)}$ provide a lower bound on the smallest eigenvalue of the neutral and charged inverse propagators, respectively. Finally, recall the large- y scaling (and that y has dimensions of mass) $\Omega_{\mathbf{k}} \sim y$. Introducing a dimensionless Yukawa coupling $Y = ya$, the mass scales as Ya^{-1} . The continuum limit is $N \rightarrow \infty$, $a \equiv L_{\text{phys}}/N$, with fixed system volume L_{phys}^2 .

In Figure 15, we display $N \min_{\mathbf{k}} \Omega_{\mathbf{k}}^{(1)}$ —the lower bound on the minimal value of the neutral fermion eigenvalue—as a function of h for $\kappa = 0.5$ and $N = 4, 8, 16$. Figure 16 displays the corresponding quantity for the charged fermions. In Figures 17 and 18, respectively, we show the lower bound on the neutral and charged eigenvalues for $\kappa = 0.1$. In units of $L_{\text{phys}}^{-1} Y$, the lower bound on the mass can be obtained by multiplying the plotted value of by the dimensionless large Yukawa coupling Y .

The numerical results for the lower bounds on the neutral and charged fermion propagator eigenvalues, μ_i , displayed in these figures, imply that:

- The lower bounds on both the neutral and charged eigenvalues μ_i , for large Y , are $\sim Y N^\alpha L_{\text{phys}}^{-1}$, with a κ - and (more weakly) h -dependent exponent $\alpha > 0$. This presents evidence that the mirror fermions decouple from the infrared physics in the $N \rightarrow \infty$, fixed L_{phys} limit.
- It is clear, by comparing Figs. 15 and 17, that the exponent α is an increasing function κ . To better study this dependence, we have also measured $\Omega_{\mathbf{k}}^{1,2}$, for $h = 2$ and $\kappa = 0.6, 0.7, \dots, 1.4$, in addition to values that we display. We found that in the interval $0.6 \leq \kappa \leq 0.8$ the exponent $\alpha \simeq 1$ (for larger values of κ appproaching $\kappa_c \geq 1$ the susceptibilities rise with N and the spectrum begins to approach that of the broken phase, see comments below). Thus for κ in this interval, the mirror fermion masses are cutoff scale times Y .
- If the lower bound on the fermion eigenvalues is actually saturated, one can conclude from the data that the charged fermions are generally heavier than the neutral ones.

In summary, our results present evidence that there are no light states in either the neutral or the charged fermion mirror sector.

Finally, to compare with the fermion spectrum in the broken phase, the dashed lines on each figure show the minimum values of Ω for $N = 4, 8, 16$, calculated to leading order in perturbation theory (strictly valid when $\kappa \rightarrow \infty$) in the broken phase. This was done by using the broken phase propagator of eqn. (B.9). As already mentioned, these perturbative results are in excellent quantitative agreement with Monte Carlo simulations in the quasi-ordered phase (performed for $\kappa = 10 \gg \kappa_c \simeq 1$). The dips in the dashed lines correspond to the approximate solutions of (B.10), leading at finite N to almost massless modes.¹¹ Our results, discussed above, show that in the symmetric phase the corresponding massless modes are absent.

Acknowledgements

EP thanks Bob Holdom for useful discussions and suggestions. JG expresses appreciation for extensive use of the FTPI computer cluster, and technical help from Graham Allan. JG was supported in part by the Department of Energy grant DE-FG02-94ER40823 at the University of Minnesota. EP is supported by the National Science and Engineering Research Council of Canada; he also gratefully acknowledges the hospitality of the Galileo Galilei Institute of Theoretical Physics in Florence during the initial stages of this work.

Appendices

A Expansion of spinors in terms of chiral GW eigenvectors and chiral split of the measure

In this Appendix, we derive an expansion of spinors in terms of Neuberger's operator eigenstates. This is useful in writing the chiral split of the measure in Section 3.2. We denote the Neuberger operator by D , obeying $\{\gamma_5, D\} = D\gamma_5 D$ and $\gamma_5 D \gamma_5 = D^\dagger$. Recall that the eigenvalues λ of D obey $\lambda + \lambda^* = \lambda\lambda^*$ and thus lie on a unit circle in the complex plane centered at 1. For every eigenvalue with $\text{Im } \lambda \neq 0$ there is another eigenvalue λ^* whose eigenvector, a 2-component spinor, is $\Psi_{\lambda^*} = \gamma_5 \Psi_\lambda$. Here $D\Psi_\lambda = \lambda\Psi_\lambda$. The inner product notation we use is $(\Psi_{\lambda'}^\dagger, \Psi_\lambda) \equiv \sum_x \Psi_{\lambda'}^\dagger{}_x \Psi_{\lambda}{}_x = \delta_{\lambda', \lambda}$. Orthogonality of eigenvectors with different eigenvalues follows from hermiticity of $\gamma_5 D$. Chiral components for the unbarred fields Ψ are defined in the usual way, $\Psi_\pm = P_\pm \Psi$, while for the barred $\bar{\Psi}$, $\bar{\Psi}_\pm = \bar{\Psi} \hat{P}_\mp$, where $\hat{P}_\pm = (1 \pm \hat{\gamma}_5)/2$, with $\hat{\gamma}_5 = (1 - D)\gamma_5$.

To define the Dirac fermion measure, we first expand an arbitrary spinor configuration in terms of the eigenvectors $\Psi_{\lambda}{}_x$ of D as follows:¹²

$$\Psi_x = \sum_{\text{Im } \lambda > 0} [c_\lambda \Psi_{\lambda}{}_x + c_{\lambda^*} \Psi_{\lambda^*}{}_x], \quad (\text{A.1})$$

¹¹We caution against concluding from the plots that the broken phase massless modes indicated in (B.10) are not present in the continuum limit for some values of h —it is easy to check that as N becomes large, the dips completely overcome the N enhancement from the scaling of y , as the eigenvalues become closely spaced on the unit circle.

¹²Here and below, there is an implicit sum over multiplicities associated with a given eigenvalue λ .

where c_λ are Grassmann numbers.¹³ The measure of the Ψ integration is, therefore:

$$\prod_x d\Psi_x = \prod_{Im\lambda>0} dc_\lambda dc_{\lambda^*} . \quad (\text{A.2})$$

The contributions of the real eigenvalues $\lambda = 0, 2$ are to be added both to (A.1) and (A.2). We note that there is no Jacobian in eqn. (A.2). This follows from the fact that the GW operator is normal ($[D^\dagger, D] = 0$) and hence can be diagonalized by a unitary transformation; the Jacobians from Ψ and $\bar{\Psi}$ transforms cancel, for any gauge field background.

Our next goal is to rewrite the measure (A.2) in terms of chiral components. This is easily accomplished for the unbarred field Ψ_x (keeping in mind that $\Psi_{\lambda^*} = \gamma_5 \Psi_\lambda$). Explicitly, we rewrite (A.1) as follows:

$$\begin{aligned} \Psi_x &= \sum_{Im\lambda>0} \left[\frac{c_\lambda + c_{\lambda^*}}{\sqrt{2}} \frac{\Psi_{\lambda x} + \Psi_{\lambda^* x}}{\sqrt{2}} + \frac{c_\lambda - c_{\lambda^*}}{\sqrt{2}} \frac{\Psi_{\lambda x} - \Psi_{\lambda^* x}}{\sqrt{2}} \right] \\ &= \sum_{Im\lambda>0} [\alpha_{\lambda+} \Psi_{\lambda+ x} + \alpha_{\lambda-} \Psi_{\lambda- x}] , \end{aligned} \quad (\text{A.3})$$

where we defined:

$$\alpha_{\lambda\pm} \equiv \frac{c_\lambda \pm c_{\lambda^*}}{\sqrt{2}} \quad (\text{A.4})$$

$$\Psi_{\lambda\pm x} \equiv \frac{\Psi_{\lambda x} \pm \Psi_{\lambda^* x}}{\sqrt{2}} . \quad (\text{A.5})$$

Now we can use the relation (A.4) to express the measure (A.2) in terms of the variables α_\pm , with a Jacobian that is only a numerical factor:

$$\prod_x d\Psi_x = \prod_{Im\lambda>0} dc_\lambda dc_{\lambda^*} = \prod_{Im\lambda>0} 4 d\alpha_{\lambda-} d\alpha_{\lambda+} \quad (\text{A.6})$$

and the expansion (A.3) to express the action in terms of the chiral integration variables α_\pm . The zero and cutoff ($\lambda = 2$) modes are easily added to (A.3), (A.6), as shown below.

Now consider the more interesting $\bar{\Psi}$ case. Note the following chain of relations: $D\Psi_\lambda = \lambda\Psi_\lambda \rightarrow \Psi_\lambda^\dagger D^\dagger = \Psi_\lambda^\dagger \lambda^* \rightarrow \Psi_\lambda^\dagger \gamma_5 D \gamma_5 = \Psi_\lambda^\dagger \lambda^* \rightarrow \Psi_{\lambda^*}^\dagger D \gamma_5 = \Psi_{\lambda^*}^\dagger \lambda^* \rightarrow \lambda^* \Psi_{\lambda^*}^\dagger \gamma_5 = \lambda^* \Psi_\lambda^\dagger$, where the γ_5 hermiticity of D was used. We continue by expanding the row spinor $\bar{\Psi}$ in terms of a complete set of Ψ_λ^\dagger solutions as follows:

$$\bar{\Psi}_x = \sum_{Im\lambda>0} [\bar{c}_\lambda \Psi_{\lambda x}^\dagger + \bar{c}_{\lambda^*} \Psi_{\lambda^* x}^\dagger] , \quad (\text{A.7})$$

again omitting the contribution of the $\lambda = 0, 2$ eigenvalues that should be always added in ones mind. Similar to (A.2) we define the barred fermion measure:

$$\prod_x d\bar{\Psi}_x \equiv \prod_{Im\lambda>0} d\bar{c}_\lambda d\bar{c}_{\lambda^*} \quad (\text{A.8})$$

¹³ Here, we have displayed the contribution of only the eigenvalues $\lambda \neq 0, 2$; the contribution of the eigenvectors of the real eigenvalues $\lambda = 0$ and $\lambda = 2$ are implicitly assumed present and will be added later. The reason is that they are always (anti)chiral in the usual sense: for $\lambda = 0, 2$ the GW chirality is equal, up to a sign, to the usual γ_5 chirality. In the free case of zero gauge background we will explicitly find these eigenvectors and see that the $\lambda = 0$ ones (one $+$ and one $-$) corresponds to $\vec{k} = (N, N)$, while the $\lambda = 2$ ones (one pair of \pm each) are obtained for the three values of momentum $\vec{k} = (N/2, N), (N, N/2), (N/2, N/2)$.

The set of relations above (A.7) are useful because they allow us to rewrite (A.7) in terms of \hat{P}_\pm components as follows:

$$\begin{aligned}\bar{\Psi}_{\pm x} \equiv (\bar{\Psi} \hat{P}_\mp)_x &= \sum_{Im\lambda > 0} \left[\bar{c}_\lambda \frac{\Psi_{\lambda x}^\dagger \mp \Psi_{\lambda^* x}^\dagger (1 - \lambda)}{2} + \bar{c}_{\lambda^*} \frac{\Psi_{\lambda^* x}^\dagger \mp \Psi_{\lambda x}^\dagger (1 - \lambda^*)}{2} \right] \\ &= \sum_{Im\lambda > 0} \frac{\bar{c}_\lambda \mp (1 - \lambda^*) \bar{c}_{\lambda^*}}{\sqrt{2}} \frac{\Psi_{\lambda x}^\dagger \mp \Psi_{\lambda^* x}^\dagger (1 - \lambda)}{\sqrt{2}},\end{aligned}\quad (\text{A.9})$$

where the first line was obtained by applying the projector to (A.7) and in the second we used $|1 - \lambda| = 1$. Thus, similar to the definition of α_\pm of (A.4), we can define:

$$\begin{aligned}\bar{\alpha}_{\lambda\pm} &= \frac{1}{\sqrt{2}} (\bar{c}_\lambda \mp (1 - \lambda^*) \bar{c}_{\lambda^*}) \\ \bar{\Psi}_{\lambda\pm x} &= \frac{1}{\sqrt{2}} \left(\Psi_{\lambda x}^\dagger \mp \Psi_{\lambda^* x}^\dagger (1 - \lambda) \right),\end{aligned}\quad (\text{A.10})$$

We see from the above equation that the Jacobian of the transformation from \bar{c} to $\bar{\alpha}_\pm$ variables depends on λ ; explicitly, eqn. (A.8) becomes:

$$\prod_x d\bar{\Psi}_x \equiv \prod_{Im\lambda > 0} d\bar{c}_\lambda d\bar{c}_{\lambda^*} = \prod_{Im\lambda > 0} 4(1 - \lambda^*) d\bar{\alpha}_{\lambda-} d\bar{\alpha}_{\lambda+}. \quad (\text{A.11})$$

As a simple demonstration of the self-consistency of this procedure, we check that in the vectorlike case we can use the measure in the final form (A.6) and (A.11) to calculate the determinant of D . To this end, write first the expansion of $\bar{\Psi}$ in terms of α_\pm :

$$\bar{\Psi}_x = \sum_{Im\lambda > 0} \frac{\bar{\alpha}_{\lambda+} + \bar{\alpha}_{\lambda-}}{\sqrt{2}} \Psi_{\lambda x}^\dagger + \frac{\bar{\alpha}_{\lambda+} - \bar{\alpha}_{\lambda-}}{\sqrt{2}(\lambda^* - 1)} \Psi_{\lambda^* x}^\dagger, \quad (\text{A.12})$$

(recalling that zero and cutoff modes should be added as well) also note that the $\lambda^* - 1$ factor in the denominator does not vanish since $\lambda = 1$ is not in the spectrum. Then, substitute (A.12) as well as the α_\pm expansion of Ψ of eqn. (A.3) into the GW action to obtain, using the orthogonality of the Ψ_λ wavefunctions and recalling that $\lambda = \lambda^*/(\lambda^* - 1)$:

$$(\bar{\Psi}, D\Psi) \equiv \sum_x \bar{\Psi}_x (D\Psi)_x = \sum_{Im\lambda > 0} \bar{\alpha}_{\lambda+} \alpha_{\lambda+} \lambda + \bar{\alpha}_{\lambda-} \alpha_{\lambda-} \lambda. \quad (\text{A.13})$$

Now recall the $\bar{\alpha}_\pm$ measure (A.11) and the similar expression (A.6) (with constant Jacobian) for Ψ to find that the path integral over the $\lambda \neq 0, 2$ eigenvalues reduces to

$$\begin{aligned}\int \prod_x d\Psi_x d\bar{\Psi}_x e^{(\bar{\Psi}, D\Psi)} &= c \prod_{Im\lambda > 0} \lambda^2 (1 - \lambda^*) = c' \prod_{Im\lambda > 0} \lambda \lambda^* \\ &= c' \prod_{\lambda \neq 0, 2} \lambda = c' \det(D)|_{\lambda \neq 0, 2},\end{aligned}\quad (\text{A.14})$$

i.e. the determinant of D , as appropriate (the factor c' hides various numerical constants as well as the contributions of the $\lambda = 0, 2$ eigenvalues). The point of this exercise was to show that the Jacobian factor in (A.11) was crucial to obtaining the right result.

We end this section by summarizing the important formulae that were derived: the expansions of the fermionic fields in terms of generalized chiral and antichiral Grassmann amplitudes $\alpha_{\pm}, \bar{\alpha}_{\pm}$:

$$\Psi_x = \sum_{Im\lambda > 0} \left[\frac{\alpha_{\lambda+} + \alpha_{\lambda-}}{\sqrt{2}} \Psi_{\lambda x} + \frac{\alpha_{\lambda+} - \alpha_{\lambda-}}{\sqrt{2}} \Psi_{\lambda^* x} \right] \quad (\text{A.15})$$

$$\bar{\Psi}_x = \sum_{Im\lambda > 0} \left[\frac{\bar{\alpha}_{\lambda+} + \bar{\alpha}_{\lambda-}}{\sqrt{2}} \Psi_{\lambda x}^{\dagger} + \frac{\bar{\alpha}_{\lambda+} - \bar{\alpha}_{\lambda-}}{\sqrt{2}(\lambda^* - 1)} \Psi_{\lambda^* x}^{\dagger} \right] \quad (\text{A.16})$$

and an expression for the measure, combining (A.6) and (A.11), in terms of these Grassmann amplitudes:

$$\prod_x d\bar{\Psi}_x d\Psi_x \equiv c \prod_{Im\lambda > 0} d\alpha_{\lambda+} d\alpha_{\lambda-} d\bar{\alpha}_{\lambda+} d\bar{\alpha}_{\lambda-} (1 - \lambda^*) . \quad (\text{A.17})$$

This defines a split of the measure in terms of chiral and antichiral fields. The zero and cutoff modes (the real eigenvalues of D) should be added to (A.15, A.16, A.17).

The usefulness of (A.15, A.16) is that if we write the lagrangian in terms of $\Psi_{\pm}, \bar{\Psi}_{\pm}$ components, e.g., as in (3.15), we have a straightforward way to express the corresponding terms via the integration variables α_{\pm} . For example, if a term contains $\bar{\Psi}_{+x}$, we simply need use (A.16) and put all $\bar{\alpha}_{-}$ to zero in that expansion, etc.

A.1 Explicit form for the GW eigenvectors for $g = 0$.

Here we work out the explicit form of the eigenvectors of the Neuberger-Dirac operator in the free case. We begin by writing the free Neuberger-Dirac operator in momentum space:

$$\Psi_x = \frac{1}{N} \sum_{k_1, k_2=1}^N \omega_N^{\vec{k} \cdot \vec{x}} \tilde{\Psi}(k) , \quad \omega_N \equiv e^{\frac{2\pi i}{N}} , \quad (\text{A.18})$$

$$(D\Psi)_x = \frac{1}{N} \sum_{k_1, k_2=1}^N \omega_N^{\vec{k} \cdot \vec{x}} D(\mathbf{k}) \tilde{\Psi}(k) . \quad (\text{A.19})$$

We also define $s_{\mu} \equiv \sin(\pi k_{\mu}/N)$ and $c_{\mu} \equiv \cos(\pi k_{\mu}/N)$ and the following functions of $k_{\mu} = 1, \dots, N$, $\mu = 1, 2$:

$$\begin{aligned} a_{\mathbf{k}} &\equiv 1 - \frac{1 - 2s_1^2 - 2s_2^2}{\sqrt{1 + 8s_1^2 s_2^2}} , \\ b_{\mathbf{k}} &\equiv \frac{2s_2 c_2}{\sqrt{1 + 8s_1^2 s_2^2}} , \\ c_{\mathbf{k}} &\equiv \frac{2s_1 c_1}{\sqrt{1 + 8s_1^2 s_2^2}} , \end{aligned} \quad (\text{A.20})$$

in terms of which $D(\mathbf{k})$ takes the explicit form (we use $\gamma_1 = \sigma_1, \gamma_2 = \sigma_2, \gamma_5 = \sigma_3$):

$$D(\mathbf{k}) = \begin{pmatrix} a_{\mathbf{k}} & ic_{\mathbf{k}} + b_{\mathbf{k}} \\ ic_{\mathbf{k}} - b_{\mathbf{k}} & a_{\mathbf{k}} \end{pmatrix} . \quad (\text{A.21})$$

The GW condition is equivalent to the relation $a_{\mathbf{k}}^2 + b_{\mathbf{k}}^2 + c_{\mathbf{k}}^2 = 2a_{\mathbf{k}}$, which is easily verified from (A.20). The eigenvalues of $D(\mathbf{k})$ are:

$$\lambda_{\mathbf{k}} = a_{\mathbf{k}} \pm i\sqrt{b_{\mathbf{k}}^2 + c_{\mathbf{k}}^2}. \quad (\text{A.22})$$

With the help of this equation it is easily seen that the only real eigenvalues occur for $\mathbf{k} = (N, N), (N/2, N), (N, N/2)$ and $(N/2, N/2)$. The (N, N) eigenvalue is the zero mode $\lambda = 0$, while the other three correspond to the cutoff value $\lambda = 2$. For every one of these eigenvalues there are two eigenvectors of opposite γ_5 chirality; these can be taken simply to be represented by $\begin{pmatrix} 0 \\ 1 \end{pmatrix}$ and $\begin{pmatrix} 1 \\ 0 \end{pmatrix}$, as will be done explicitly in eqn. (A.27).

The eigenvectors with $\text{Im}\lambda > 0$ are explicitly given by:

$$\Psi_{\lambda_{\mathbf{k}} x} = \frac{1}{\sqrt{2}N} \omega_N^{\vec{k} \cdot \vec{x}} \begin{pmatrix} 1 \\ \frac{ib_{\mathbf{k}} + c_{\mathbf{k}}}{\sqrt{b_{\mathbf{k}}^2 + c_{\mathbf{k}}^2}} \end{pmatrix}, \quad (\text{A.23})$$

and are easily seen to obey:

$$\left(\Psi_{\lambda_{\mathbf{k}}}^\dagger, \Psi_{\lambda_{\mathbf{k}'}} \right) \equiv \sum_{\vec{x}} \Psi_{\lambda_{\mathbf{k}} x}^\dagger \Psi_{\lambda_{\mathbf{k}'} x} = \delta_{\vec{k}, \vec{k}'}, \quad (\text{A.24})$$

a property assumed in deriving, e.g. (A.13, A.14). In particular, the expansions (A.15, A.16, A.17) hold by simply replacing the Ψ_λ there by (A.23); note that the sums and products there are over all \vec{k} apart from the four points corresponding to real eigenvalues.

Now consider the $\lambda = 2$ eigenvalues; the $\lambda = 0$ ones can be considered in exact parallel. We proceed simply by recalling that $\lambda = 2$ eigenvalues are always (anti)chiral in the usual sense. More precisely, for the unbarred spinors, GW and usual chirality coincide for any λ , while for the barred spinors, GW and usual chirality are opposite for $\lambda = 2$; this simply follows from the fact that for $\lambda = 2$ we have $\hat{\gamma}_5 = (1 - D)\gamma_5 = -\gamma_5$. In our basis of gamma matrices definite γ_5 chirality Ψ_\pm spinors have the form:

$$\Psi_+ = \begin{pmatrix} a \\ 0 \end{pmatrix}, \quad \Psi_- = \begin{pmatrix} 0 \\ b \end{pmatrix}, \quad (\text{A.25})$$

while definite $\hat{\gamma}_5 = -\gamma_5$ chirality $\bar{\Psi}_\pm$ are $\bar{\Psi}_\pm \equiv \bar{\Psi} \hat{P}_\mp = \bar{\Psi}(1 \mp \hat{\gamma}_5)/2|_{\lambda=2} = \bar{\Psi}(1 \pm \gamma_5)/2$. Thus, the $\bar{\Psi}_\pm$ spinors with $\lambda = 2$ have the form:

$$\bar{\Psi}_+ = (c \ 0), \quad \bar{\Psi}_- = (0 \ d). \quad (\text{A.26})$$

This allows us to write the $\lambda = 2$ solutions for two spinors Ψ_- and Ψ_+ (we use the fact that $\lambda = 2$ solutions in the free case occur for $\vec{k} = (N/2, N/2), (N, N/2), (N/2, N)$ only):

$$\begin{aligned} \Psi_{-x} &= \frac{1}{N} \left(\omega_N^{(N/2)x_1 + (N/2)x_2} \alpha_- + \omega_N^{(N/2)x_1 + Nx_2} \beta_- + \omega_N^{Nx_1 + (N/2)x_2} \gamma_- \right) \begin{pmatrix} 0 \\ 1 \end{pmatrix} \\ \Psi_{+x} &= \frac{1}{N} \left(\omega_N^{(N/2)x_1 + (N/2)x_2} \alpha_+ + \omega_N^{(N/2)x_1 + Nx_2} \beta_+ + \omega_N^{Nx_1 + (N/2)x_2} \gamma_+ \right) \begin{pmatrix} 1 \\ 0 \end{pmatrix} \\ \bar{\Psi}_{-x} &= \frac{1}{N} \left(\omega_N^{-(N/2)x_1 - (N/2)x_2} \bar{\alpha}_- + \omega_N^{-(N/2)x_1 - Nx_2} \bar{\beta}_- + \omega_N^{-Nx_1 - (N/2)x_2} \bar{\gamma}_- \right) (0 \ 1) \\ \bar{\Psi}_{+x} &= \frac{1}{N} \left(\omega_N^{-(N/2)x_1 - (N/2)x_2} \bar{\alpha}_+ + \omega_N^{-(N/2)x_1 - Nx_2} \bar{\beta}_+ + \omega_N^{-Nx_1 - (N/2)x_2} \bar{\gamma}_+ \right) (1 \ 0), \end{aligned} \quad (\text{A.27})$$

where the α, β, γ are the corresponding Grassmann integration variables of the $\lambda = 2$ modes; also clearly the various position factors are either unity or of the form $(-1)^{x_1}$, etc., which will be important when performing the summations after the further insertion in the action.

Now, we put all formulae together, using the momentum space eigenvectors of $D(\mathbf{k})$ found above, to obtain the final form of the expansion of $\Psi, \bar{\Psi}$ in terms of GW eigenvectors. To this end, we first define the phase factor from the eigenvectors (A.23), now extended to include all \mathbf{k} :

$$e^{i\varphi_{\mathbf{k}}} \equiv \begin{cases} \frac{ib_{\mathbf{k}} + c_{\mathbf{k}}}{\sqrt{b_{\mathbf{k}}^2 + c_{\mathbf{k}}^2}} & \text{if } \mathbf{k} \neq (N, N), (\frac{N}{2}, N), (N, \frac{N}{2}), (\frac{N}{2}, \frac{N}{2}) \\ 1 & \text{if } \mathbf{k} = (N, N), (\frac{N}{2}, N), (N, \frac{N}{2}), (\frac{N}{2}, \frac{N}{2}) \end{cases}, \quad (\text{A.28})$$

and introduce the unitary matrices $U_{\mathbf{k}}$ and $V_{\mathbf{k}}$:

$$U_{\mathbf{k}} = \frac{1}{2} \begin{pmatrix} 2 - \lambda_{\mathbf{k}} & \lambda_{\mathbf{k}} e^{-i\varphi_{\mathbf{k}}} \\ -\lambda_{\mathbf{k}}^* e^{i\varphi_{\mathbf{k}}} & 2 - \lambda_{\mathbf{k}}^* \end{pmatrix}, \quad V_{\mathbf{k}} = \frac{1}{2} \begin{pmatrix} (2 - \lambda_{\mathbf{k}}^*) e^{i\varphi_{\mathbf{k}}} & -\lambda_{\mathbf{k}}^* \\ \lambda_{\mathbf{k}} & (2 - \lambda_{\mathbf{k}}) e^{-i\varphi_{\mathbf{k}}} \end{pmatrix}. \quad (\text{A.29})$$

Then, the final result for the momentum-space expansion of the GW-chirality components of the Dirac spinors is:

$$\begin{aligned} \Psi_{-x} &= \frac{1}{N} \sum_{\mathbf{k}=1}^N \alpha_{\mathbf{k}-} \omega_N^{\mathbf{k} \cdot \mathbf{x}} e^{-i\varphi_{\mathbf{k}} \sigma_3} \begin{pmatrix} 0 \\ 1 \end{pmatrix}, \\ \Psi_{+x} &= \frac{1}{N} \sum_{\mathbf{k}=1}^N \alpha_{\mathbf{k}+} \omega_N^{\mathbf{k} \cdot \mathbf{x}} \begin{pmatrix} 1 \\ 0 \end{pmatrix}, \\ \bar{\Psi}_{-x} &= \frac{1}{N} \sum_{\mathbf{k}=1}^N \bar{\alpha}_{\mathbf{k}-} \omega_N^{-\mathbf{k} \cdot \mathbf{x}} \begin{pmatrix} 1 & 0 \end{pmatrix} U_{\mathbf{k}}, \\ \bar{\Psi}_{+x} &= \frac{1}{N} \sum_{\mathbf{k}=1}^N \bar{\alpha}_{\mathbf{k}+} \omega_N^{-\mathbf{k} \cdot \mathbf{x}} \begin{pmatrix} 0 & 1 \end{pmatrix} V_{\mathbf{k}}. \end{aligned} \quad (\text{A.30})$$

We note again that the barred spinors are treated as two-component rows, as explicitly evident in the above expansions. The sum in (A.30) is over all momenta and thus includes also the real eigenvalues of the GW operator. Note also that $U_{\mathbf{k}} = \sigma_3 V_{\mathbf{k}}^* e^{i\sigma_3 \varphi_{\mathbf{k}}} \sigma_3$ and that the chiral projectors for the $\bar{\Psi}$ fields can be written in terms of $U_{\mathbf{k}}, V_{\mathbf{k}}$:

$$\hat{P}_{\pm \mathbf{k}} = U_{\mathbf{k}}^\dagger P_{\pm} U_{\mathbf{k}} = V_{\mathbf{k}}^\dagger P_{\pm} V_{\mathbf{k}} \quad (\text{A.31})$$

In this notation, the fact that as $\mathbf{k} \rightarrow \mathbf{0}$ the usual and GW chirality coincide is evident—in this limit, the unitary matrices $U_{\mathbf{k}}, V_{\mathbf{k}}$ become the identity.

B Fermion Green functions

B.1 Neutral fermion Green functions

As explained in the main text, see eqn. (3.36), we define the following fermion observable, appropriate in the large y limit, when only correlators between left and right fields are nonzero:

$$S_{x-y}^m = \begin{pmatrix} \langle \chi_{+x} \phi_y \psi_{-y}^T \rangle & \langle \chi_{+x} \phi_y^* \bar{\psi}_{-y} \rangle \\ \langle \bar{\chi}_{+x}^T \phi_y \psi_{-y}^T \rangle & \langle \bar{\chi}_{+x}^T \phi_y^* \bar{\psi}_{-y} \rangle \end{pmatrix} \quad (\text{B.1})$$

These correlators probe the spectrum of neutral fermions—as explained in the Introduction, the charged fermions ψ_- can bind with the charged scalars into neutral fermions, which then pair up with the neutral mirrors to form massive states; see the strong coupling expansions in [13, 14] for discussion of analogous phenomena.

Then define, for every value of k , the four-by-four matrix propagator in momentum space, and use the expressions (A.30) (χ_+ is obtained by replacing $\alpha_+ \rightarrow \beta_+$ in the corresponding equation in (A.30)):

$$\begin{aligned} s_{\mathbf{k}}^n &= \sum_x \omega_N^{-\mathbf{k}(x-y)} S_{x-y}^n \\ &= \sum_{\mathbf{p}} \begin{pmatrix} \langle \beta_{\mathbf{k}} \alpha_{\mathbf{p}} \Phi_{-\mathbf{k}-\mathbf{p}} \rangle e^{i\varphi_{\mathbf{p}}} \sigma_+ & \langle \beta_{\mathbf{k}} \bar{\alpha}_{\mathbf{k}+\mathbf{p}} \Phi_{\mathbf{p}}^* \rangle P_+ U_{\mathbf{k}+\mathbf{p}} \\ \langle \bar{\beta}_{-\mathbf{k}} \alpha_{\mathbf{p}-\mathbf{k}} \Phi_{-\mathbf{p}} \rangle V_{-\mathbf{k}}^T P_- e^{i\varphi_{\mathbf{p}-\mathbf{k}}} & \langle \bar{\beta}_{-\mathbf{k}} \bar{\alpha}_{\mathbf{p}} \Phi_{\mathbf{p}-\mathbf{k}}^* \rangle V_{-\mathbf{k}}^T \sigma_- U_{\mathbf{p}} \end{pmatrix}. \end{aligned} \quad (\text{B.2})$$

Here, (A.29) defines the U and V matrices and $e^{i\varphi}$ is defined in (A.28). We will study numerically the following quantity:

$$\Omega_{\mathbf{k}}^{(1)} = \frac{1}{\sqrt{\text{Tr } s_{\mathbf{k}}^n {}^\dagger s_{\mathbf{k}}^n}}, \quad (\text{B.3})$$

which, as discussed in Section 3.4, provides a lower bound on the smallest neutral fermion inverse propagator eigenvalue.

It is instructive to consider the form of the neutral Green functions for constant $\phi_x = 1$ background, where they can be evaluated explicitly. This is, of course, only relevant for large values of κ where the fluctuations of ϕ_x are nearly frozen. Note that for $\phi_x = 1$ there is no difference between the charged and neutral Green functions (defined in following section). The propagator $s_{\mathbf{k}}$ then takes the form:

$$s_{\mathbf{k}}^0 = \begin{pmatrix} \langle \beta_{\mathbf{k}} \alpha_{-\mathbf{k}} \rangle \sigma_+ e^{i\varphi_{-\mathbf{k}}} & \langle \beta_{\mathbf{k}} \bar{\alpha}_{\mathbf{k}} \rangle P_+ U_{\mathbf{k}} \\ \langle \bar{\beta}_{-\mathbf{k}} \alpha_{-\mathbf{k}} \rangle V_{-\mathbf{k}}^T P_- e^{i\varphi_{-\mathbf{k}}} & \langle \bar{\beta}_{-\mathbf{k}} \bar{\alpha}_{\mathbf{k}} \rangle V_{-\mathbf{k}}^T \sigma_- U_{\mathbf{k}} \end{pmatrix}. \quad (\text{B.4})$$

The biunitary transform of $s_{\mathbf{k}}^0$:

$$\hat{s}_{\mathbf{k}}^0 \equiv \begin{pmatrix} 1 & 0 \\ 0 & V_{-\mathbf{k}}^* \end{pmatrix} s_{\mathbf{k}}^0 \begin{pmatrix} 1 & 0 \\ 0 & U_{\mathbf{k}}^\dagger \end{pmatrix}, \quad (\text{B.5})$$

takes the even simpler form:

$$\hat{s}_{\mathbf{k}}^0 = \begin{pmatrix} \langle \beta_{\mathbf{k}} \alpha_{-\mathbf{k}} \rangle \sigma_+ e^{i\varphi_{-\mathbf{k}}} & \langle \beta_{\mathbf{k}} \bar{\alpha}_{\mathbf{k}} \rangle P_+ \\ \langle \bar{\beta}_{-\mathbf{k}} \alpha_{-\mathbf{k}} \rangle P_- e^{i\varphi_{-\mathbf{k}}} & \langle \bar{\beta}_{-\mathbf{k}} \bar{\alpha}_{\mathbf{k}} \rangle \sigma_- \end{pmatrix} \quad (\text{B.6})$$

and makes explicit the fact that the rank of the matrix is two, the number of propagating complex degrees of freedom. The relevant expectation values entering the Green functions can be easily computed for constant ϕ_x and are given by (it is important to take into account the measure factor

$1 - \lambda_{\mathbf{k}}^*$ (3.20) when calculating the expectation values):

$$\begin{aligned}
\langle \beta_{\mathbf{k}} \alpha_{-\mathbf{k}} \rangle &= -i h e^{-i\varphi_{\mathbf{k}}} \frac{4 - 4\lambda_{\mathbf{k}} + 2\lambda_{\mathbf{k}}^2}{4} d(\mathbf{k})^{-1} \\
\langle \beta_{\mathbf{k}} \bar{\alpha}_{\mathbf{k}} \rangle &= \frac{2 - \lambda_{\mathbf{k}}^*}{2} d(\mathbf{k})^{-1} \\
\langle \bar{\beta}_{-\mathbf{k}} \bar{\alpha}_{\mathbf{k}} \rangle &= -i h e^{i\varphi_{\mathbf{k}}} (1 - \lambda_{\mathbf{k}}^*) d(\mathbf{k})^{-1} \\
\langle \bar{\beta}_{-\mathbf{k}} \alpha_{-\mathbf{k}} \rangle &= -\frac{2 - \lambda_{\mathbf{k}}}{2} d(\mathbf{k})^{-1} ,
\end{aligned} \tag{B.7}$$

where

$$d(\mathbf{k}) = \sin^2 \frac{\theta_{\mathbf{k}}}{2} + h^2 \cos \theta_{\mathbf{k}}, \quad \lambda_{\mathbf{k}} \equiv 1 + e^{i\theta_{\mathbf{k}}} . \tag{B.8}$$

Combining (B.6, B.7) we find:

$$\hat{s}_{\mathbf{k}}^0 = \frac{1}{d(\mathbf{k})} \begin{pmatrix} -i h \frac{4-4\lambda_{\mathbf{k}}+2\lambda_{\mathbf{k}}^2}{4} e^{i(\varphi_{-\mathbf{k}}-\varphi_{\mathbf{k}})} \sigma_+ & \frac{2-\lambda_{\mathbf{k}}^*}{2} P_+ \\ -\frac{2-\lambda_{\mathbf{k}}}{2} e^{i\varphi_{-\mathbf{k}}} P_- & -i h e^{i\varphi_{\mathbf{k}}} (1-\lambda_{\mathbf{k}}^*) \sigma_- \end{pmatrix} . \tag{B.9}$$

The rank of $\hat{s}_{\mathbf{k}}^0$ is two; clearly, the nontrivial part is obtained by simply replacing σ_{\pm} and P_{\pm} by unity. After the elimination of two rows and columns of zeros, the determinant of $\hat{s}_{\mathbf{k}}^0$ equals $e^{i\varphi_{-\mathbf{k}}} d(\mathbf{k})^{-1}$. Clearly, the denominator (B.8) of $\hat{s}_{\mathbf{k}}^0$ admits small eigenvalues for values of \mathbf{k} where (assuming $h > 1/2$):

$$\left| \sin \frac{\theta_{\mathbf{k}}}{2} \right| = \frac{h}{\sqrt{2h^2 - 1}} . \tag{B.10}$$

For generic values of h this equation has no exact solutions at finite N , except for $h = 0$, where the $\theta_{\mathbf{k}} = 0$ corresponds to the three unlifted modes with $\lambda_{\mathbf{k}} = 2$, and $h = 1$, corresponding to $\theta_{\mathbf{k}} = \pi$, where the $\mathbf{k} = (N, N)$ mode is unlifted. Other values of \mathbf{k} for which (B.10) approximately holds occur, for sufficiently large h near $\theta_{\mathbf{k}} \simeq \frac{\pi}{2}$, and give rise to small mass eigenvalues in the broken phase.

As explained in the main text below (3.22), the $h = 1$ exact zero mode persists for small κ as well. It gives rise to the critical behavior seen in our numerical analysis at $h \approx 1$, and discussed in the main body of the paper.

As a consistency check on our numerical simulations, we have also verified that for large values of κ , in the algebraically ordered phase, where perturbation theory leading to (B.9) is valid, the mass matrix, including the small eigenvalues due to (B.10), are reproduced by our Monte-Carlo simulations.

Most importantly, however, as described in the main text, in the disordered phase with rapid fluctuations of ϕ_x , our results for $\Omega_{\mathbf{k}}^{1,2}$ show that there are no small eigenvalues in the $h > 1$ regime.

B.2 Charged fermion Green functions

The correlators that probe the charged fermion spectrum, eqn. (3.31), where charged bound states of the neutral mirrors χ_+ and the scalars can pair up with the charged mirrors to form heavy fermions, appropriate to the large- y limit are as follows:

$$S_{y-x}^c = \begin{pmatrix} \langle \psi_{-x} \chi_{+y}^T \phi_y \rangle & \langle \chi_{+x} \phi_x^* \bar{\psi}_{-y} \rangle \\ \langle \psi_{-x} \bar{\chi}_{+y} \phi_y \rangle & \langle \bar{\chi}_{+x}^T \phi_x^* \bar{\psi}_{-y} \rangle \end{pmatrix} \tag{B.11}$$

For every value of k , the four-by-four matrix propagator in momentum space is, then, similar to (B.2):

$$\begin{aligned} s_{\mathbf{k}}^c &= \sum_x \omega_N^{-\mathbf{k}(x-y)} S_{x-y}^c \\ &= \sum_{\mathbf{p}} \begin{pmatrix} \langle \alpha_{\mathbf{k}} \beta_{\mathbf{p}} \Phi_{-\mathbf{k}-\mathbf{p}} \rangle e^{i\varphi_{\mathbf{k}}} \sigma_- & \langle \beta_{\mathbf{p}} \bar{\alpha}_{\mathbf{k}} \Phi_{\mathbf{k}-\mathbf{p}}^* \rangle P_+ U_{\mathbf{k}} \\ \langle \alpha_{\mathbf{k}} \bar{\beta}_{\mathbf{p}} \Phi_{\mathbf{p}-\mathbf{k}} \rangle P_- V_{\mathbf{p}} e^{i\varphi_{\mathbf{k}}} & \langle \bar{\alpha}_{\mathbf{k}} \bar{\beta}_{\mathbf{p}} \Phi_{\mathbf{p}+\mathbf{k}}^* \rangle V_{\mathbf{p}}^T \sigma_- U_{\mathbf{k}} \end{pmatrix}. \end{aligned} \quad (\text{B.12})$$

The quantity that we numerically study is defined as for the neutral propagator (B.3):

$$\Omega_{\mathbf{k}}^{(2)} = \frac{1}{\sqrt{\text{Tr } s_{\mathbf{k}}^c{}^\dagger s_{\mathbf{k}}^c}}, \quad (\text{B.13})$$

and similarly provides a lower bound on the smallest eigenvalue of the inverse charged-fermion propagator.

B.3 Fermion-bilinear susceptibilities

There are two composite charged complex scalars that we can construct out of bilinears of the mirror fermions— $\bar{\psi}_{-x} \chi_{+x}$ and $\psi_{-x}^T \gamma_2 \chi_{+x}$. Consider the corresponding susceptibilities:

$$\Delta_{x-y} \equiv \langle \bar{\psi}_{-x} \chi_{+x} \bar{\chi}_{+y} \psi_{-y} \rangle \quad (\text{B.14})$$

$$= \frac{1}{N^4} \sum_{\mathbf{k}, \mathbf{p}, \mathbf{q}, \mathbf{l}} \langle \bar{\alpha}_{\mathbf{k}} \beta_{\mathbf{p}} \bar{\beta}_{\mathbf{q}} \alpha_{\mathbf{l}} \rangle \omega_N^{(\mathbf{p}-\mathbf{k})x} \omega_N^{(\mathbf{l}-\mathbf{q})y} \frac{(2-\lambda_{\mathbf{k}})(2-\lambda_{\mathbf{q}})}{4} e^{i(\varphi_{\mathbf{l}}-\varphi_{\mathbf{q}})}. \quad (\text{B.15})$$

We now define a susceptibility as in the scalar case:

$$\chi_F \equiv \sum_x \Delta_{x-y}|_{\text{connected}} \quad (\text{B.16})$$

$$= \frac{1}{N^2} \sum_{\mathbf{k}, \mathbf{q}} \frac{(2-\lambda_{\mathbf{k}})(2-\lambda_{\mathbf{q}})}{4} (\langle \bar{\alpha}_{\mathbf{k}} \beta_{\mathbf{k}} \bar{\beta}_{\mathbf{q}} \alpha_{\mathbf{q}} \rangle - \langle \bar{\alpha}_{\mathbf{k}} \beta_{\mathbf{k}} \rangle \langle \bar{\beta}_{\mathbf{q}} \alpha_{\mathbf{q}} \rangle), \quad (\text{B.17})$$

where we subtracted the disconnected component, which should vanish anyway in the symmetric phase (we have checked that it, indeed, does vanish). Consider also the "Majorana" correlator:

$$\Delta'_{x-y} \equiv \langle \psi_{-x}^T \gamma_2 \chi_{+x} \bar{\chi}_{+y} \gamma_2 \bar{\psi}_{-y}^T \rangle \quad (\text{B.18})$$

$$= -\frac{1}{4N^4} \sum_{\mathbf{k}, \mathbf{p}, \mathbf{q}, \mathbf{l}} \langle \alpha_{\mathbf{k}} \beta_{\mathbf{p}} \bar{\beta}_{\mathbf{q}} \bar{\alpha}_{\mathbf{l}} \rangle e^{i\varphi_{\mathbf{k}}} \omega_N^{(\mathbf{k}+\mathbf{p})x} \omega_N^{-(\mathbf{q}+\mathbf{l})y} ((2-\lambda_{\mathbf{q}})(2-\lambda_{\mathbf{l}})e^{-i\varphi_{\mathbf{q}}} - \lambda_{\mathbf{q}}\lambda_{\mathbf{l}}e^{-i\varphi_{\mathbf{l}}}),$$

and the corresponding "Majorana susceptibility:"

$$\chi'_F \equiv \sum_x \Delta'_{x-y}|_{\text{connected}} \quad (\text{B.19})$$

$$= -\frac{1}{4N^2} \sum_{\mathbf{k}, \mathbf{q}} e^{i(\varphi_{\mathbf{k}}-\varphi_{\mathbf{q}})} (4-4\lambda_{\mathbf{q}}+2\lambda_{\mathbf{q}}^2) (\langle \alpha_{\mathbf{k}} \beta_{-\mathbf{k}} \bar{\beta}_{\mathbf{q}} \bar{\alpha}_{-\mathbf{q}} \rangle - \langle \alpha_{\mathbf{k}} \beta_{-\mathbf{k}} \rangle \langle \bar{\beta}_{\mathbf{q}} \bar{\alpha}_{-\mathbf{q}} \rangle),$$

where, again, we subtracted the disconnected part, which (as we checked, once more) vanishes in the symmetric phase.

N	h	κ	Metropolis	Wolff + det RW
4	4	0.1	1.423(5)	1.424(8)
4	2	0.5	3.65(4)	3.57(4)
8	4	0.1	1.026(4)	1.021(8)

Table 2: Sample comparison points, Metropolis results versus Wolff algorithm with determinant reweighting.

C Simulation details

The configurations of XY fields η are generated using the Wolff single-cluster algorithm [40], which is well-known to overcome critical slowing down for this lattice system. The fermion measure is taken into account through determinant reweighting:

$$\langle \mathcal{O} \rangle = \frac{\langle \mathcal{O} \det M \rangle_\eta}{\langle \det M \rangle_\eta}. \quad (\text{C.1})$$

Here, \mathcal{O} is any observable, and $\langle \cdots \rangle_\eta$ denotes an expectation value with respect to the measure of the XY model (cf. eq. (2.11) with $U \equiv 1$),

$$d\mu(\eta) = Z_{XY}^{-1} \left(\prod_x d\eta_x \right) \exp(-S_\kappa). \quad (\text{C.2})$$

We monitor the reliability of this method in three ways.

1. We measure the autocorrelation time for reweighted quantities $\langle \mathcal{O} \det M \rangle_\eta$, as well as $\langle \det M \rangle_\eta$, to be certain that the configurations remain independent with respect to the new measure.
2. We perform a jackknife error analysis of the averages $\langle \mathcal{O} \rangle$ that are obtained, gathering sufficient data to keep errors small. (An “overlap problem” would be indicated by large errors.)
3. We have simulated a number of sample points in parameter space by an alternative method that does not rely on determinant reweighting. Namely, we have used Metropolis updates that include $\Delta S = -\ln \det M$ in the action. We check that this alternative (significantly slower, due to much longer autocorrelation times that occur when using the Metropolis algorithm) method leads to results that agree with the determinant reweighting method. Sample comparison points are presented in Table 2.

We find that the Wolff cluster algorithm together with determinant reweighting is efficient and reliable for all quantities and regions of parameter space that we have explored. The only difficulty that occurs is a sign problem in the $h < 1$ regime, as mentioned in the main text. However, this is easy to detect due to the associated large statistical errors.

C.1 Comments on $y^{-1} \neq 0$

To include $y < \infty$ in our simulations, we have to work with a Pfaffian, as is clear from the results of Section (3.2), eqns. (3.17, 3.22). A method to compute the Pfaffian, including the phase,

is found in the appendix of ref. [42]. We want to determine the sign ambiguity that occurs in $\text{Pf } \mathcal{M} = \pm \det \mathcal{M}^{1/2}$, since it is obviously crucial to any averaging; here, we denoted by \mathcal{M} the fermion matrix determined by eqns. (3.17, 3.22) at $y < \infty$. Similarly, we denote by M the fermion matrix in the $y \rightarrow \infty$ limit.

For $y^{-1} \lesssim 10^{-3}$, we find that $\ln \text{Pf } \mathcal{M} = \ln \det M$ to within 4 or 5 digits for $N = 4$ and $N = 8$ lattices. That is so close that it will not change any of the results that were stated in Sections (3.3, 3.4) above. The result $\ln \text{Pf } \mathcal{M} = \ln \det M$ does not appear to depend on the lattice size.

Right at $h = 1$, M becomes singular for arbitrary ϕ backgrounds and there is an increased sensitivity to the y^{-1} corrections.

Returning to $h \neq 1$, here are some more empirical results. For $y^{-1} \gtrsim 0.1$, $\text{Pf } \mathcal{M}$ is noticeably different from $\det M$. However, the complex phase seems much less sensitive to y^{-1} corrections than the magnitude. The complex phase of $\text{Pf } \mathcal{M}$ does fluctuate a bit from configuration to configuration. But for $y = 10$, it is a fluctuation in the fourth significant digit—hardly a “complex phase problem.”

References

- [1] P. H. Ginsparg and K. G. Wilson, “A remnant of chiral symmetry on the lattice,” *Phys. Rev. D* **25**, 2649 (1982).
- [2] D. B. Kaplan, “A method for simulating chiral fermions on the lattice,” *Phys. Lett. B* **288**, 342 (1992) [arXiv:hep-lat/9206013].
- [3] R. Narayanan and H. Neuberger, “Chiral fermions on the lattice,” *Phys. Rev. Lett.* **71**, 3251 (1993) [arXiv:hep-lat/9308011];
R. Narayanan and H. Neuberger, “A construction of lattice chiral gauge theories,” *Nucl. Phys. B* **443**, 305 (1995) [arXiv:hep-th/9411108].
- [4] H. Neuberger, “Exactly massless quarks on the lattice,” *Phys. Lett. B* **417**, 141 (1998) [arXiv:hep-lat/9707022].
- [5] P. Hasenfratz, V. Laliena and F. Niedermayer, “The index theorem in QCD with a finite cut-off,” *Phys. Lett. B* **427**, 125 (1998) [arXiv:hep-lat/9801021].
- [6] M. Luscher, “Exact chiral symmetry on the lattice and the Ginsparg-Wilson relation,” *Phys. Lett. B* **428**, 342 (1998) [arXiv:hep-lat/9802011].
M. Luscher, “Abelian chiral gauge theories on the lattice with exact gauge invariance,” *Nucl. Phys. B* **549**, 295 (1999) [arXiv:hep-lat/9811032].
M. Luscher, “Lattice regularization of chiral gauge theories to all orders of perturbation theory,” *JHEP* **0006**, 028 (2000) [arXiv:hep-lat/0006014].
- [7] M. Golterman, “Lattice chiral gauge theories,” *Nucl. Phys. Proc. Suppl.* **94**, 189 (2001) [arXiv:hep-lat/0011027].
- [8] M. Luscher, “Chiral gauge theories revisited,” arXiv:hep-th/0102028.
- [9] M. Golterman and Y. Shamir, “SU(N) chiral gauge theories on the lattice,” *Phys. Rev. D* **70**, 094506 (2004) [arXiv:hep-lat/0404011].

- [10] T. Bhattacharya, C. Csaki, M. R. Martin, Y. Shirman and J. Terning, “Warped domain wall fermions,” *JHEP* **0508**, 061 (2005), [arXiv:hep-lat/0503011].
- [11] R. Narayanan and H. Neuberger, “Massless composite fermions in two dimensions and the overlap,” *Phys. Lett. B* **393** (1997) 360; [*Phys. Lett. B* **402** (1997) 320] [arXiv:hep-lat/9609031];
Y. Kikukawa, R. Narayanan and H. Neuberger, “Monte Carlo evaluation of a fermion number violating observable in 2D,” *Phys. Rev. D* **57**, 1233 (1998) [arXiv:hep-lat/9705006];
Y. Kikukawa, R. Narayanan and H. Neuberger, “Finite size corrections in two dimensional gauge theories and a quantitative chiral test of the overlap,” *Phys. Lett. B* **399**, 105 (1997) [arXiv:hep-th/9701007].
- [12] T. Bhattacharya, M. R. Martin and E. Poppitz, “Chiral lattice gauge theories from warped domain walls and Ginsparg-Wilson fermions,” *Phys. Rev. D* **74**, 085028 (2006) [arXiv:hep-lat/0605003].
- [13] E. Eichten and J. Preskill, “Chiral gauge theories on the lattice,” *Nucl. Phys. B* **268**, 179 (1986).
- [14] A. Hasenfratz and T. Neuhaus, “Nonperturbative study of the strongly coupled scalar fermion model,” *Phys. Lett. B* **220**, 435 (1989).
- [15] M. A. Stephanov and M. M. Tsypin, “The phase structure of the $U(1)$ Higgs-fermion lattice theory,” *Phys. Lett. B* **242**, 432 (1990).
- [16] M. Golterman and D. N. Petcher, “The $1/d$ expansion for lattice theories of chiral fermions with Yukawa couplings,” *Nucl. Phys. B* **359**, 91 (1991).
- [17] M. Golterman, D. N. Petcher and J. Smit, “Fermion interactions in models with strong Wilson-Yukawa couplings,” *Nucl. Phys. B* **370**, 51 (1992);
W. Bock, A. K. De, E. Focht and J. Smit, “Fermion Higgs model with strong Wilson-Yukawa coupling in two dimensions,” *Nucl. Phys. B* **401**, 481 (1993) [arXiv:hep-lat/9210022].
- [18] E. Witten, “Chiral symmetry, the $1/N$ expansion, and the $SU(N)$ Thirring model,” *Nucl. Phys. B* **145**, 110 (1978).
- [19] N. D. Mermin and H. Wagner, “Absence of ferromagnetism or antiferromagnetism in one-dimensional or two-dimensional isotropic Heisenberg models,” *Phys. Rev. Lett.* **17**, 1133 (1966); S. R. Coleman, “There are no Goldstone bosons in two-dimensions,” *Commun. Math. Phys.* **31**, 259 (1973).
- [20] D. B. Kaplan, “Chiral fermions on the lattice,” *Nucl. Phys. Proc. Suppl.* **30**, 597 (1993).
- [21] M. Golterman, K. Jansen, D. N. Petcher and J. C. Vink, “Investigation of the domain wall fermion approach to chiral gauge theories on the lattice,” *Phys. Rev. D* **49**, 1606 (1994) [arXiv:hep-lat/9309015].
- [22] M. Golterman and Y. Shamir, “Domain wall fermions in a waveguide: the phase diagram at large Yukawa coupling,” *Phys. Rev. D* **51**, 3026 (1995) [arXiv:hep-lat/9409013].

- [23] C. Itzykson and J.-M. Drouffe, “Statistical field theory,” v.1 (Cambridge Univ. Press, 1989).
- [24] K. Binder, “Finite size scaling analysis of Ising model block distribution functions,” *Z. Phys. B* **43**, 119 (1981).
- [25] P. Hernandez and P. Boucaud, “A Wilson-Yukawa model with undoubled chiral fermions in 2D,” *Nucl. Phys. B* **513**, 593 (1998) [arXiv:hep-lat/9706021].
- [26] P. Hernandez and R. Sundrum, “A lattice construction of chiral gauge theories,” *Nucl. Phys. B* **455**, 287 (1995) [arXiv:hep-ph/9506331].
- [27] E. Poppitz and Y. Shang, “Lattice chirality and the decoupling of mirror fermions,” *JHEP* **08** (2007) 081, arXiv:0706.1043v2 [hep-th].
- [28] P. Gerhold and K. Jansen, “On the phase structure of a chiral invariant Higgs-Yukawa model,” arXiv:hep-lat/0610012;
P. Gerhold and K. Jansen, “The phase structure of a chirally invariant lattice Higgs-Yukawa model for small and for large values of the Yukawa coupling constant,” *JHEP* **0709**(2007)041, arXiv:0705.2539v2 [hep-lat].
- [29] P. Gerhold and K. Jansen, “The phase structure of a chirally invariant lattice Higgs-Yukawa model—numerical simulations,” *JHEP* **0710** (2007)001, arXiv:0707.3849v1 [hep-lat]
- [30] I. G. Halliday, E. Rabinovici, A. Schwimmer and M. S. Chanowitz, “Quantization of anomalous two-dimensional models,” *Nucl. Phys. B* **268**, 413 (1986).
- [31] K. Fujikawa, “A continuum limit of the chiral Jacobian in lattice gauge theory,” *Nucl. Phys. B* **546**, 480 (1999) [arXiv:hep-th/9811235].
- [32] M. Golterman and Y. Shamir, “Fermion-number violation in regularizations that preserve fermion-number symmetry,” *Phys. Rev. D* **67**, 014501 (2003) [arXiv:hep-th/0202162].
- [33] M. Creutz, M. Tytgat, C. Rebbi and S. S. Xue, “Lattice formulation of the standard model,” *Phys. Lett. B* **402**, 341 (1997) [arXiv:hep-lat/9612017].
- [34] M. Golterman, D. N. Petcher and E. Rivas, “Absence of chiral fermions in the Eichten-Preskill model,” *Nucl. Phys. B* **395**, 596 (1993) [arXiv:hep-lat/9206010].
- [35] E. H. Fradkin and S. H. Shenker, “Phase diagrams of lattice gauge theories with Higgs fields,” *Phys. Rev. D* **19**, 3682 (1979).
- [36] D. Foerster, H. B. Nielsen and M. Ninomiya, “Dynamical stability of local gauge symmetry: creation of light from chaos,” *Phys. Lett. B* **94**, 135 (1980).
- [37] P. Hernandez, K. Jansen and M. Luscher, “Locality properties of Neuberger’s lattice Dirac operator,” *Nucl. Phys. B* **552**, 363 (1999) [arXiv:hep-lat/9808010].
- [38] H. Neuberger, “Bounds on the Wilson Dirac operator,” *Phys. Rev. D* **61**, 085015 (2000) [arXiv:hep-lat/9911004].

- [39] R. Jackiw and R. Rajaraman, “Vector meson mass generation through chiral anomalies,” *Phys. Rev. Lett.* **54**, 1219 (1985) [Erratum-ibid. **54**, 2060 (1985)].
- [40] U. Wolff, “Collective Monte Carlo updating for spin systems,” *Phys. Rev. Lett.* **62** (1989) 361.
- [41] J. Tobochnik and G.V. Chester, “Monte Carlo study of the planar spin model,” *Phys. Rev. B* **20** (1979) 3761.
- [42] S. Catterall and S. Karamov, “A lattice study of the two-dimensional Wess Zumino model,” *Phys. Rev. D* **68**, 014503 (2003) [arXiv:hep-lat/0305002].

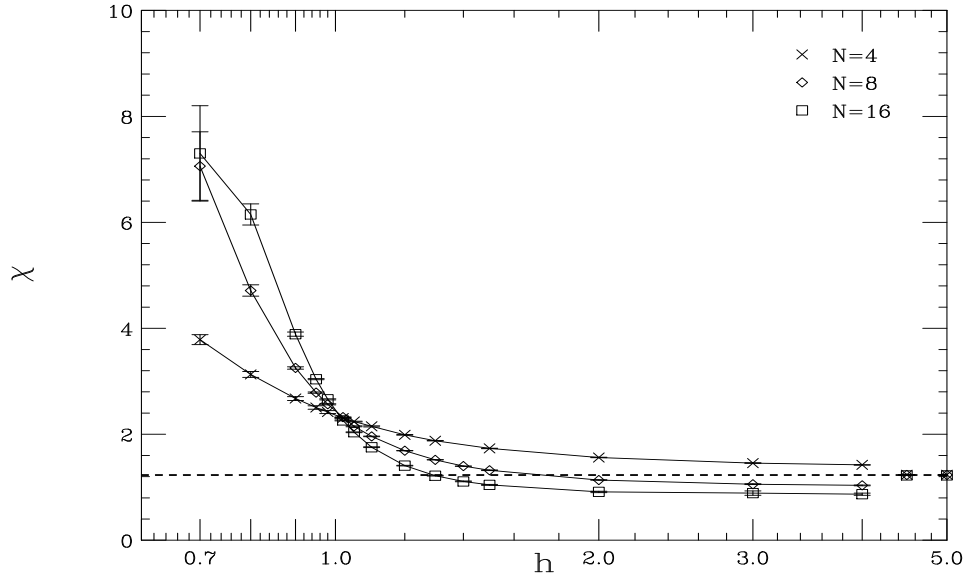


Figure 1: Comparison of susceptibilities for $\kappa = 0.1$. The dashed line indicates the susceptibilities for the pure XY model with same κ (undistinguishable, within errors for $N = 4, 8, 16$). Here and below, large errors at $h = 0.7$ and 0.8 are due to the sign problem at $h < 1$.

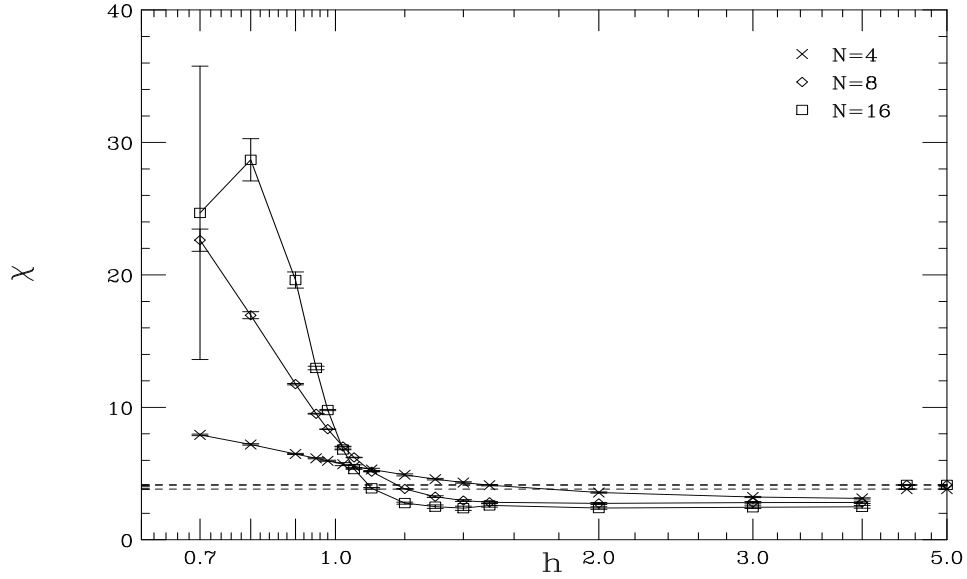


Figure 2: Comparison of susceptibilities for $\kappa = 0.5$. The dashed lines indicate the susceptibilities for the pure XY model with same κ .

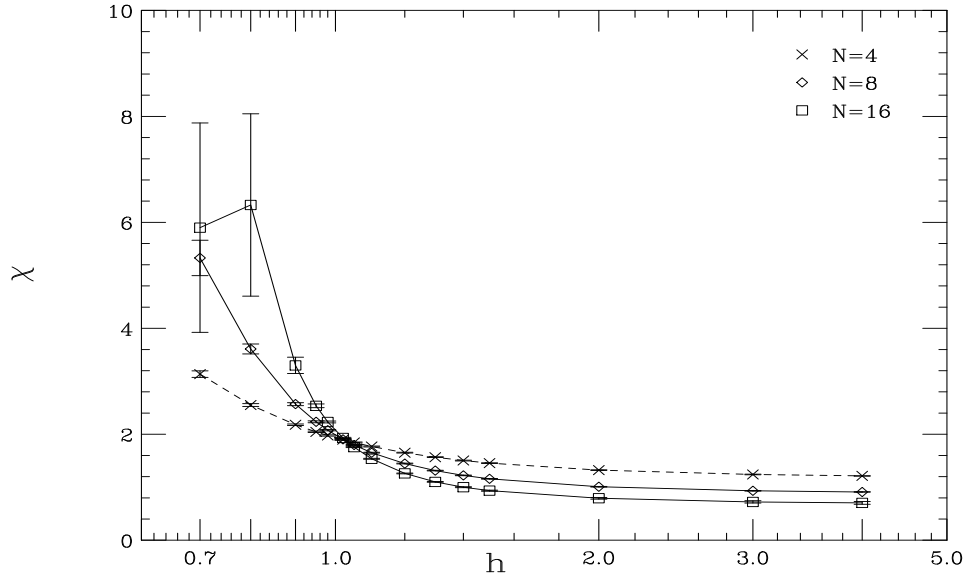


Figure 3: Comparison of susceptibilities for $\kappa = 0$. The results are qualitatively similar to those obtained for $\kappa = 0.1, 0.5$.

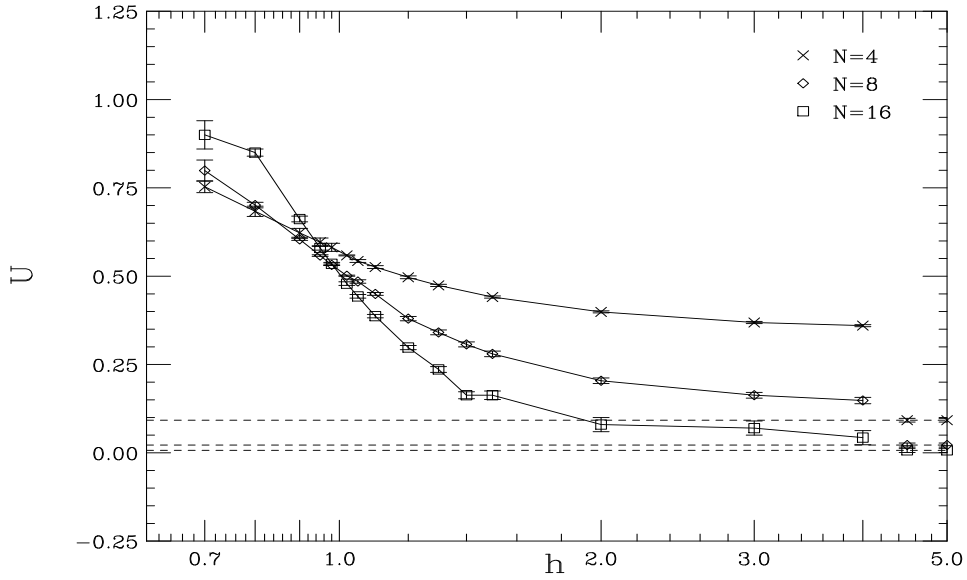


Figure 4: Comparison of Binder cumulant for $\kappa = 0.1$. The dashed lines indicate the values of the Binder cumulant for the pure XY model with same κ .

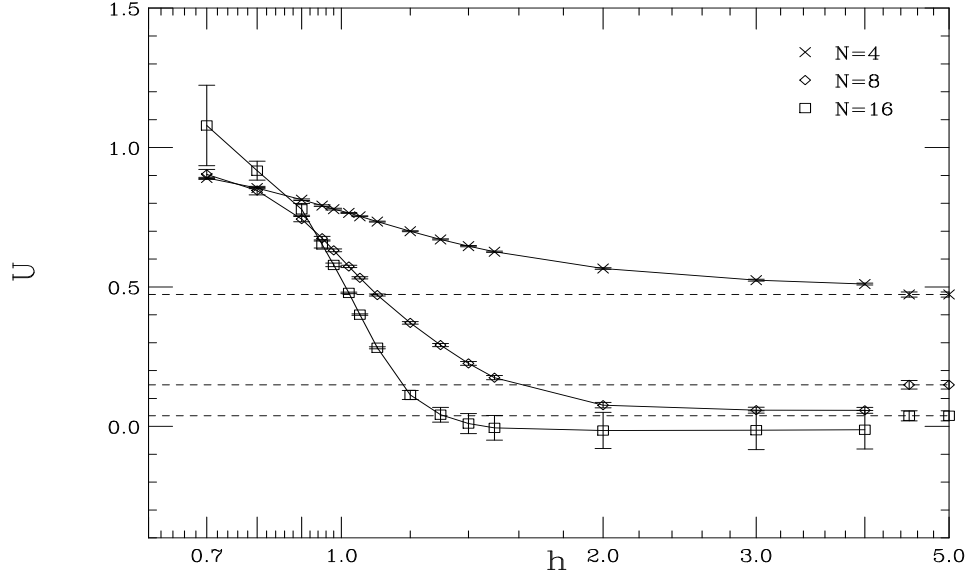


Figure 5: Comparison of Binder cumulant for $\kappa = 0.5$. The dashed lines indicate the values of the Binder cumulant for the pure XY model with the same κ .

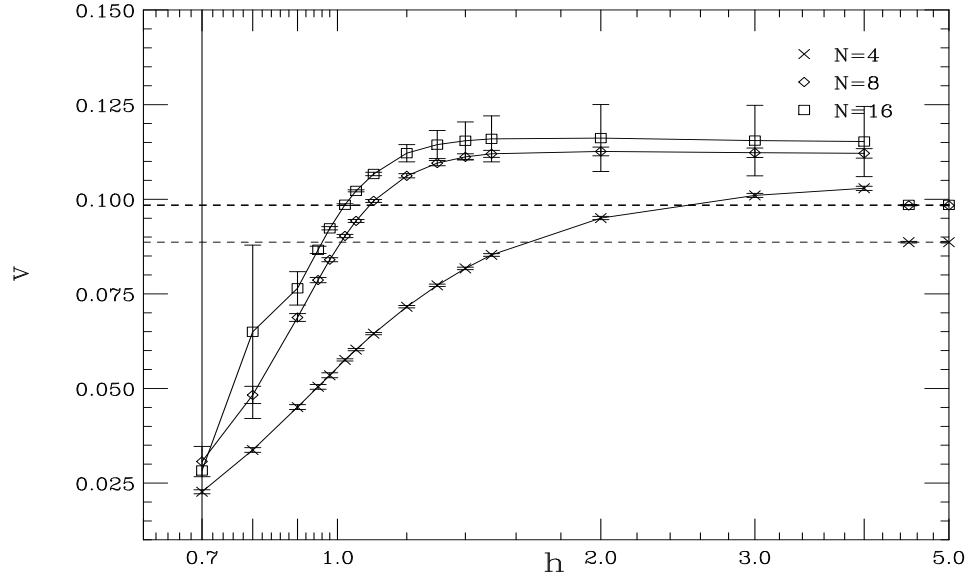


Figure 6: The vortex density for $\kappa = 0.5$ as a function of h . The pure XY model values of the vortex densities for $\kappa = 0.5$ are shown in the corresponding dashed lines. The slight increase of the vortex density at $h > 1$ (especially for $N = 8, 16$) implies that the fermions lower the vortex energy.

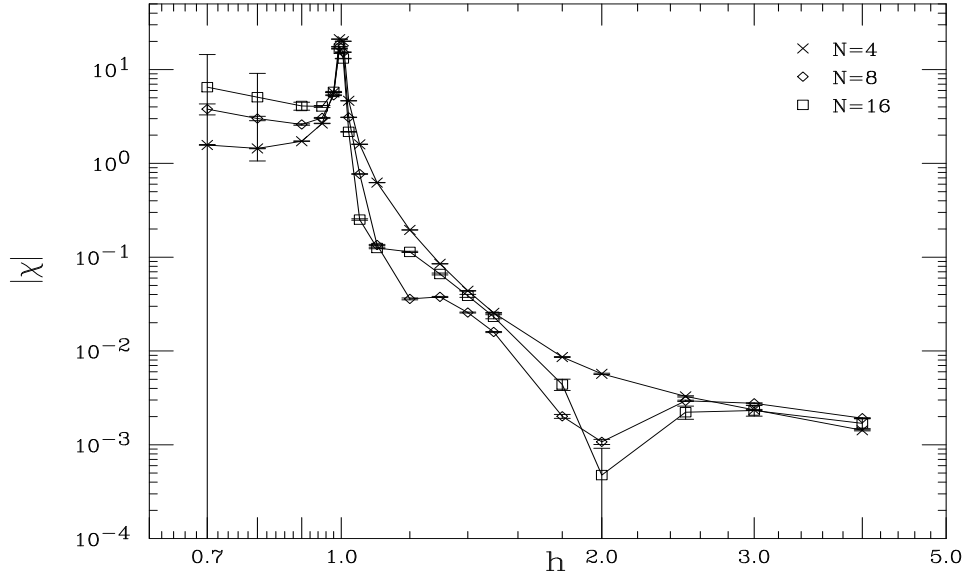


Figure 7: The magnitude of the “Dirac” susceptibility χ_F for $\kappa = 0.5$. The values of all physical susceptibilities are obtained from the plot by multiplying the plotted value by the inverse square power of the dimensionless Yukawa coupling $1/Y^2 = 1/(ay)^2$.

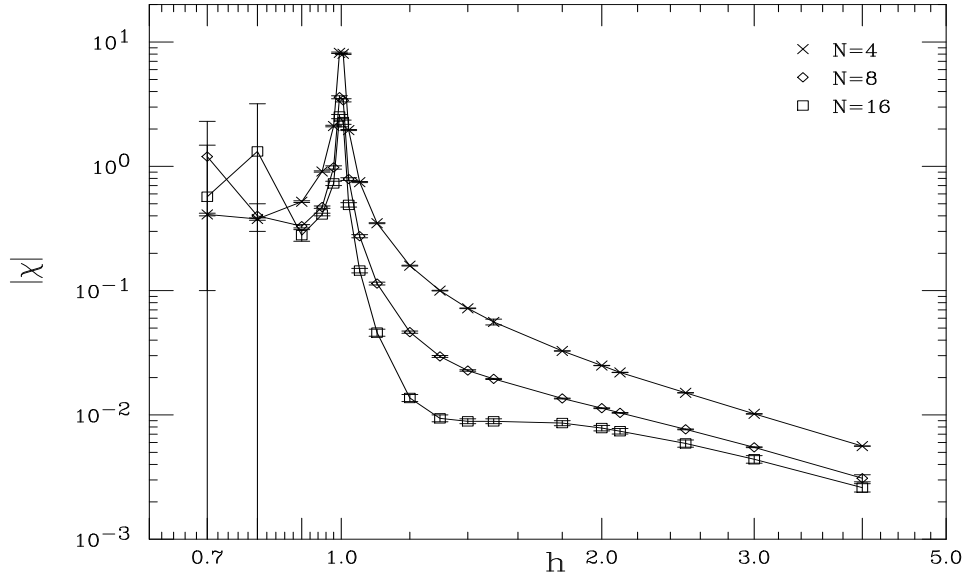


Figure 8: The magnitude of the “Dirac” susceptibility χ_F for $\kappa = 0.1$.

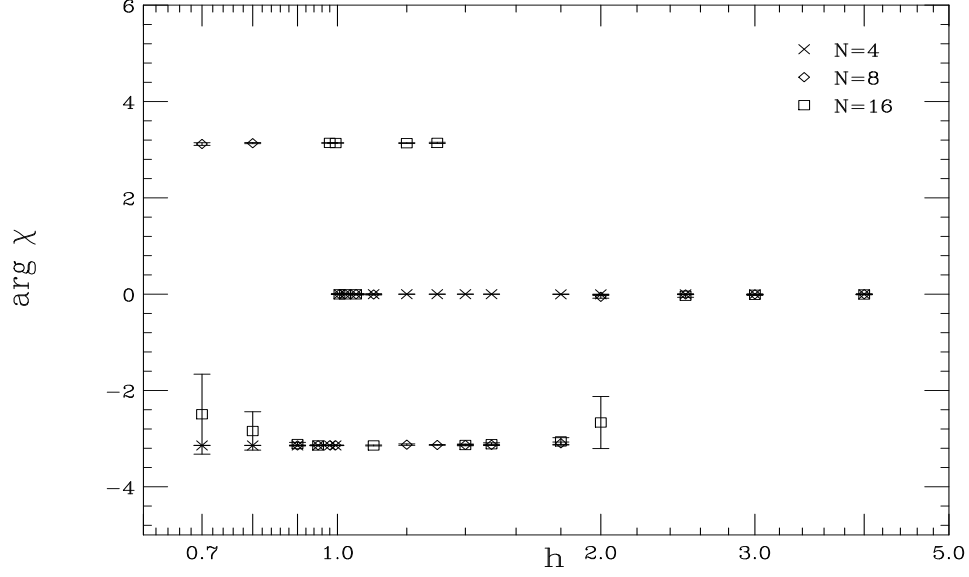


Figure 9: The argument of the “Dirac” susceptibility χ_F for $\kappa = 0.5$.

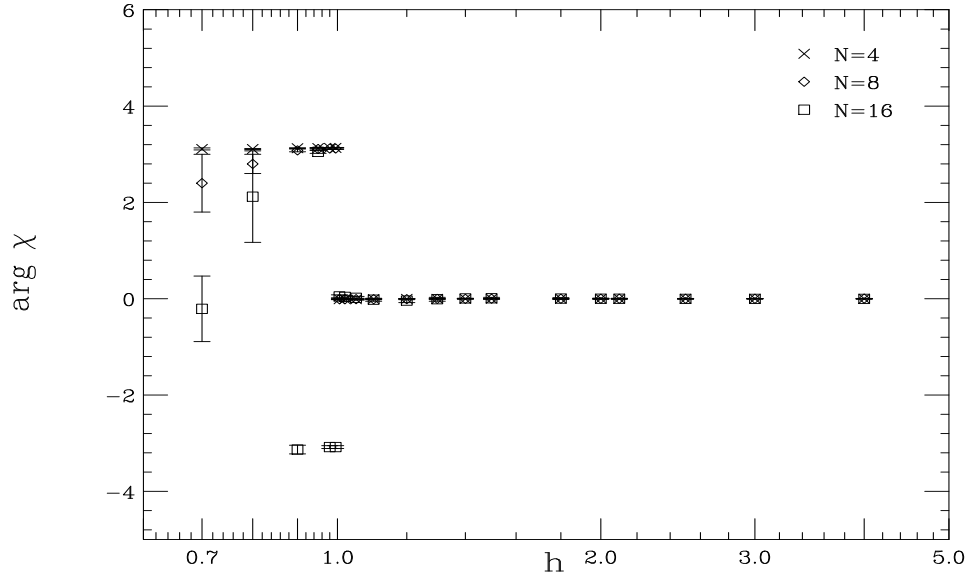


Figure 10: The argument of the “Dirac” susceptibility χ_F for $\kappa = 0.1$.

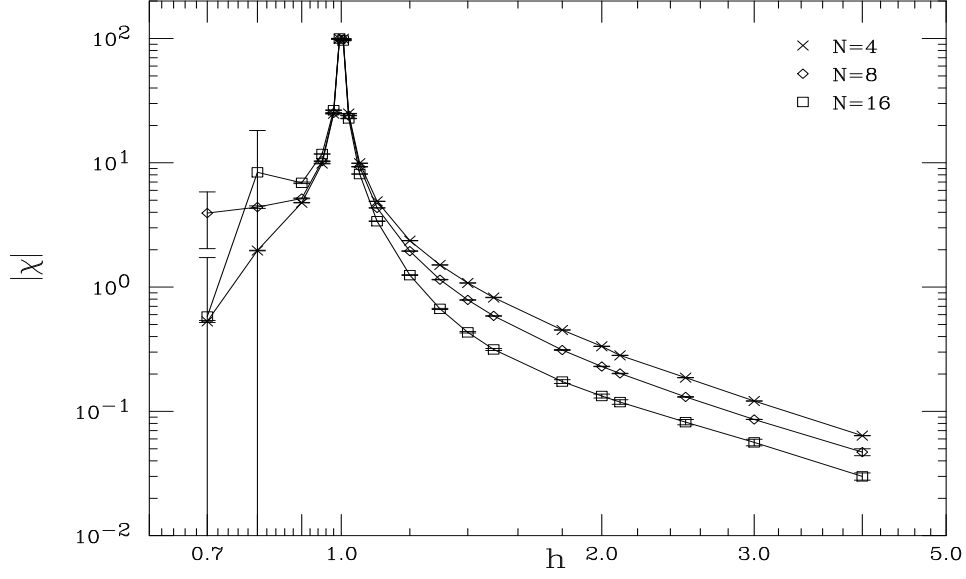


Figure 11: The magnitude of the “Majorana” susceptibility χ'_F for $\kappa = 0.1$.

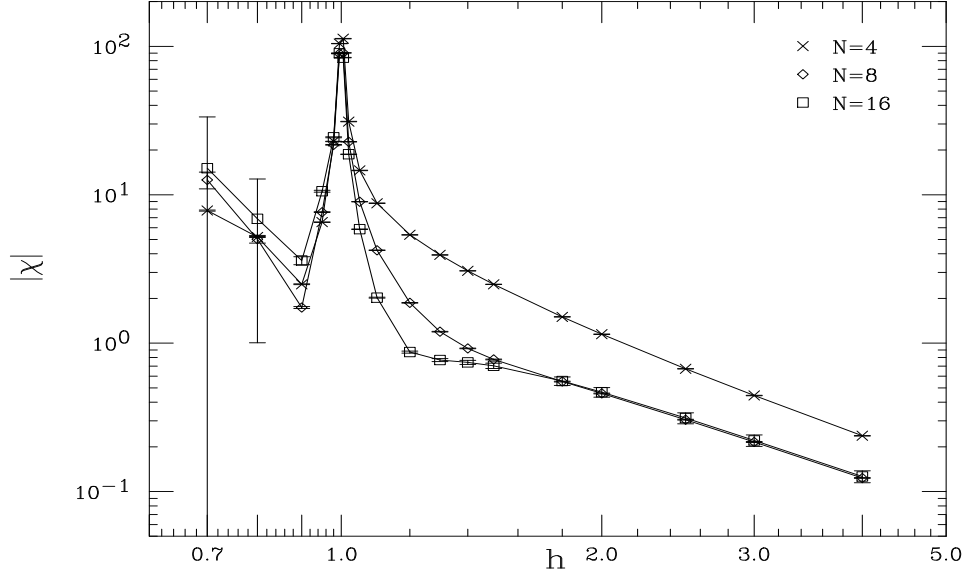


Figure 12: The magnitude of the “Majorana” susceptibility χ'_F for $\kappa = 0.5$.

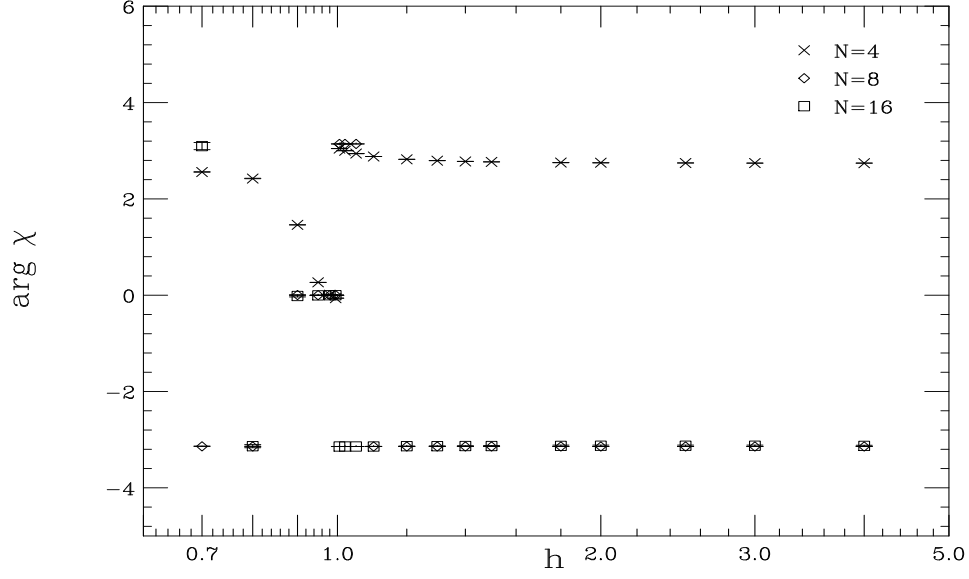


Figure 13: The argument of the “Majorana” susceptibility χ'_F for $\kappa = 0.5$.

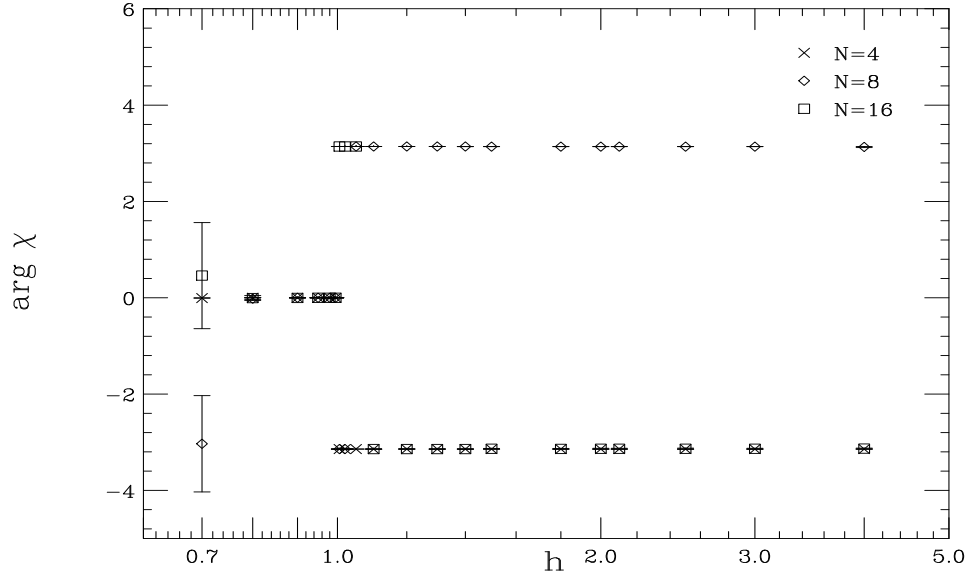


Figure 14: The argument of the “Majorana” susceptibility χ'_F for $\kappa = 0.1$.

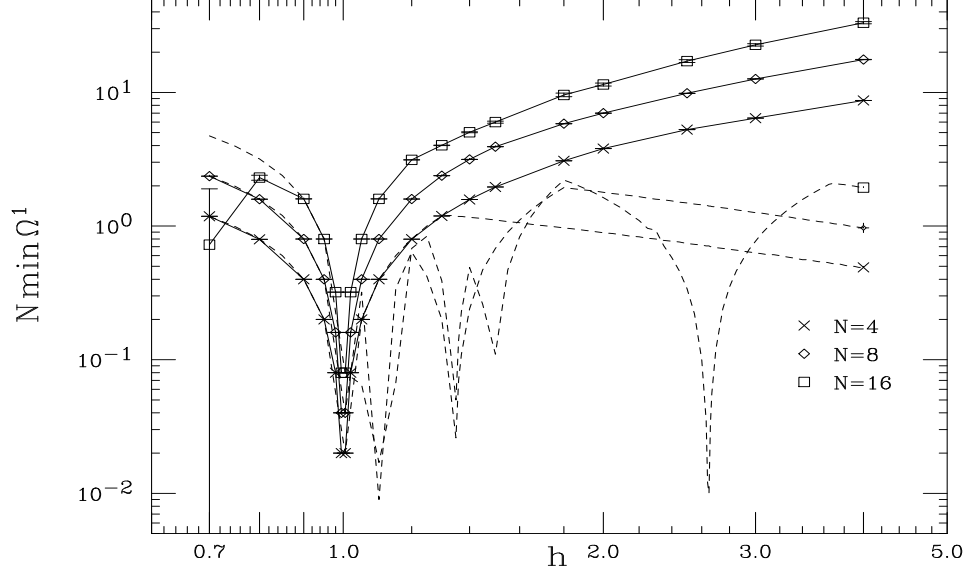


Figure 15: The lower bound on the charged mirror inverse propagator eigenvalue, $N_{\min} \Omega^1$, for $\kappa = 0.5$. The dashed lines show the same quantities in the broken ($\kappa \rightarrow \infty$) phase; their oscillations and dips are explained by eqn. (B.10). The minimum mass eigenvalues are obtained, in units of $L_{phys.}^{-1}$, by multiplying the plotted quantity by the dimensionless (large) Yukawa coupling Y ; see Section 3.4.

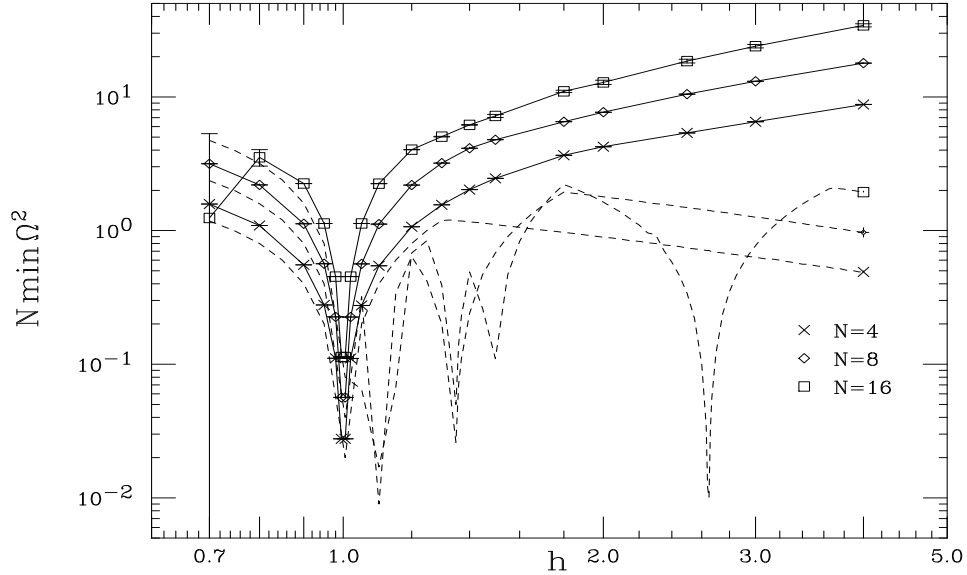


Figure 16: The lower bound on the neutral mirror fermion eigenvalue, $N_{\min} \Omega^2$, for $\kappa = 0.5$. Note that the charged fermions are heavier than the neutral in the symmetric phase.

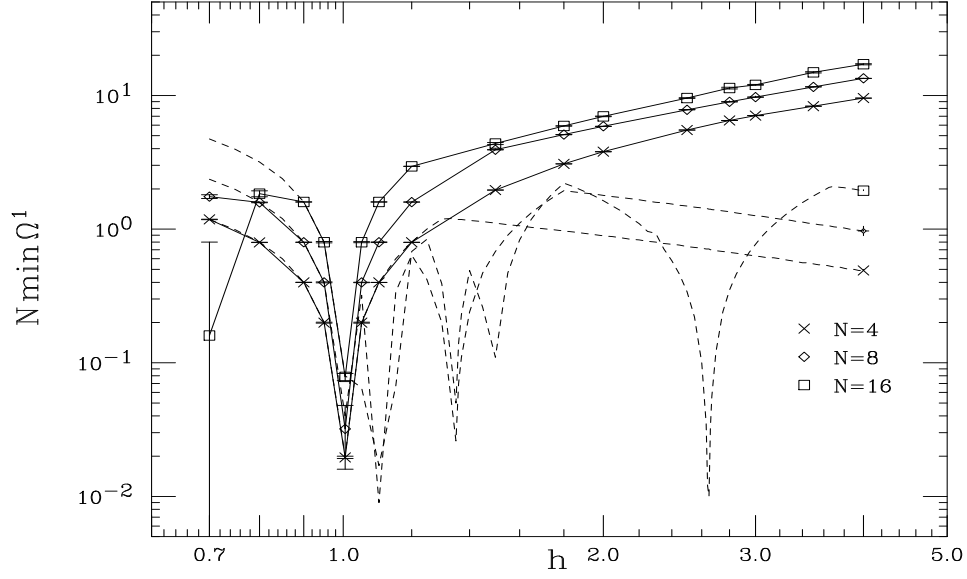


Figure 17: The lower bound on the charged mirror fermion eigenvalue, $N \min \Omega^1$, for $\kappa = 0.1$.

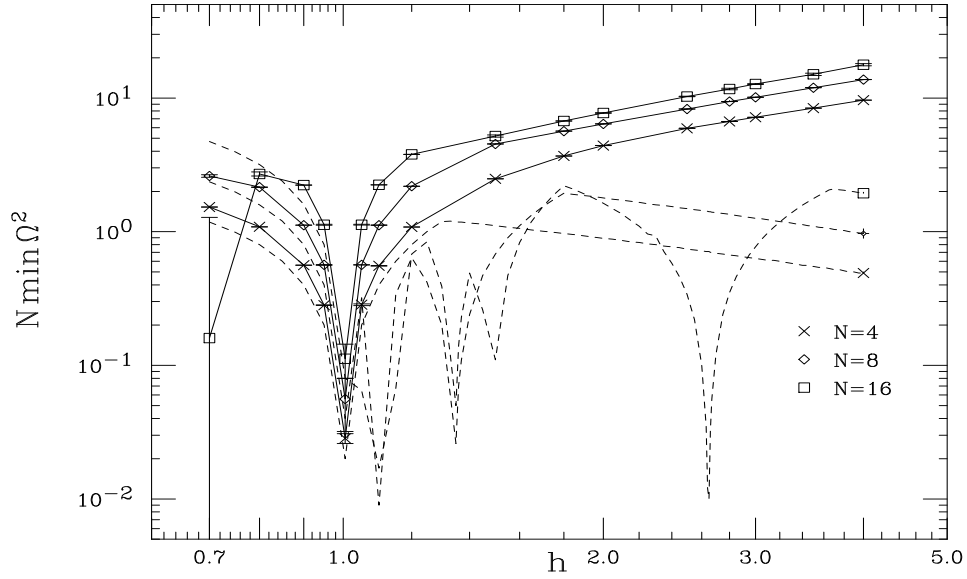


Figure 18: The lower bound on the neutral mirror fermion eigenvalue, $N \min \Omega^2$ for $\kappa = 0.1$.